

RETRIEVAL OF ATMOSPHERIC TEMPERATURE AND HUMIDITY PROFILE USING PRINCIPAL COMPONENT ANALYSIS

A PROJECT REPORT

*Submitted in partial fulfillment of the requirements
for the award of the degree of*

**BACHELOR OF TECHNOLOGY IN AEROSPACE ENGINEERING
&
MASTER OF TECHNOLOGY IN AEROSPACE ENGINEERING**

By

ABHISHEK VERMA

AE04B026

under the guidance of

Dr. C. BALAJI

Department of Mechanical Engineering

&

Dr. AMIT KUMAR

Department of Aerospace Engineering



**DEPARTMENT OF AEROSPACE ENGINEERING
INDIAN INSTITUTE OF TECHNOLOGY, MADRAS
CHENNAI – 600036**

MAY 2009

MAY 2009
THESIS CERTIFICATE

This is to certify that the thesis entitled “**Retrieval of Atmospheric Temperature and Humidity Profile Using Principal Component Analysis**” submitted by **Abhishek Verma** to the Department of Aerospace Engineering, Indian Institute of Technology, Madras, in partial fulfillment of the requirements for the award of the degree of **Bachelor of Technology** and **Master of Technology**, both, in **Aerospace Engineering** is a bonafide record of research work carried out by him under my supervision. The content of thesis, in full or in parts, has not been submitted to any other Institute or university for the award of any degree or diploma.

Dr. Amit Kumar

Project Guide

Dept. of Aerospace Engg.

IIT Madras

Dr. C. Balaji

Project Co-Guide

Dept. of Mechanical Engg.

IIT Madras

Prof. P.Sriram

Head of the Department

Dept. of Aerospace Engg.

IIT Madras

ACKNOWLEDGEMENTS

I would like to express my deep and heartfelt gratitude to a lot of people without whom I would not have succeeded in this project. First of all, I would like to thank my guide, **Dr. C. Balaji** for his guidance and support through the course of this project. Through this project, he has given me a valuable insight into research and for this I am indebted to him. His invaluable ideas and words of encouragement have always kept me motivated to give my best to this project. I would also like to thank him for his support during the hard times when the project was not going smoothly and it faced a roadblock. I wish to thank him for being more than a project guide and for mentoring me through important decisions. I also appreciate his careful review of this thesis and valuable suggestions to improve the same.

I sincerely thank **Dr. Amit Kumar** for providing the freedom and support in carrying out the project, which has always allowed me to work conveniently. I express my sincere appreciation for the faculty of the Department of Aerospace Engineering, for their intuitive teaching, supervision and guidance throughout the course of study in the department.

I would like to thank my colleagues **Vikas, Sabareesh, Gnanasekaran, Prasanna, Ashish** and **Ramanujam** for always keeping up the spirit of research with their lively and entertaining discussions.

I express my heartfelt gratitude to my special friends **Niwedita**, **Supriya**, **Eeshan** and **Rahul** for their patience and constant encouragement throughout my stay at IIT Madras. They have always been around for me and have ensured that I never lose sight of my goals. I am indebted to all my friends and all the faculty members at IIT Madras for making my stay at IIT an experience that I'll cherish all my life.

Finally, I thank my parents, my relatives and my elder sister **Manisha** for their unconditional love and motivation throughout my life and especially during my stay at IIT which allowed me to enjoy my IIT days to the fullest.

ABHISHEK VERMA

ABSTRACT

A simulations study is used to demonstrate the application of principal component analysis in retrieving climatological parameters using high spectral infrared radiances from the Atmospheric Infrared Sounder as inputs. Realistic and synthetic atmospheric profiles were used to simulate upwelling long wave radiances by 'kCompressed Atmospheric Radiative Transfer Algorithm' model. This combination of radiosonde profiles with their respective infrared radiances were utilized to derive their statistical relationships in two stages. First, principal component transform was applied to infrared radiances recorded at each channels of the sounder. Second, a feed forward back propagation type artificial neural network was used to retrieve temperature and humidity profile using reduced number of components. The number of components in input were varied in orders of 10^3 to 10^1 and performance of the algorithm was recorded. Similarly, principal component based linear regressions were carried out with same datasets and its performance was compared with neural network performance. Overall, the study concludes that principal component analysis optimizes statistical prediction of geophysical parameters. These techniques will, therefore, be a valuable tool for accurate retrieval of atmospheric parameters from new generation of Indian satellite instrument.

KEYWORD: Retrieval Algorithm, Principal Component, Artificial Neural Network, High Spectral Resolution

TABLE OF CONTENTS

	Page
ACKNOWLEDGEMENTS	i
ABSTRACT	iii
TABLE OF CONTENTS	iv
LIST OF TABLES	vi
LIST OF FIGURES	vii
NOMENCLATURE	ix

CHAPTER ONE INTRODUCTION

1.1.	BACKGROUND.....	1
1.2.	INFRARED SOUNDER.....	2
1.2.1.	Indian National Satellite System (INSAT 3D).....	3
1.2.1.	Atmospheric Infrared Sounder (AIRS).....	3
1.3.	MOTIVATION FOR THE PRESENT WORK.....	4
1.4.	CLOSURE.....	4

CHAPTER TWO REVIEW OF LITERATURE

2.1.	SUMMARY OF LITERATURE REVIEW.....	5
2.2.	CLOSURE.....	8

CHAPTER THREE MATHEMATICAL FORMULATION

3.1.	INTRODUCTION.....	9
3.2.	RADIATIVE TRANSFER EQUATION (RTE).....	9
3.2.1.	One Dimensional Radiative Transfer Equation.....	9
3.2.2.	Plane Parallel Medium Assumption.....	11
3.3.	METHODOLOGY.....	14
3.4.	CLOSURE.....	14

CHAPTER FOUR FAST FOWARD MODEL

4.1.	k COMPRESSED RADIATIVE TRANSFER ALGORITHM (kCARTA)	16
------	---	----

4.1.1.	Introduction.....	16
4.1.2.	Features of kCARTA.....	17
4.2.	CLOSURE.....	20

CHAPTER FIVE RETRIEVAL ALGORITHMS

5.1.	DATABASE FOR RETRIEVAL ALGORITHM.....	21
5.1.1.	Realistic Dataset.....	21
5.1.2.	Synthetic Profiles.....	22
5.1.3.	Training and Testing Datasets.....	25
5.2.	REGRESSION.....	26
5.3.	ARTIFICIAL NEURAL NETWORK (ANN).....	27
5.4.	PRINCIPAL COMPONENT ANALYSIS (PCA).....	30
5.5.	CLOSURE.....	36

CHAPTER SIX RESULTS AND DISCUSSION

6.1.	RETRIEVAL OF TEMPERATURE AND HUMIDITY PROFILE.....	37
6.1.1.	TYPE1 Dataset.....	37
6.1.2.	TYPE2 Dataset.....	46
6.2.	CLOSURE.....	54

CHAPTER SEVEN CONCLUSIONS AND SCOPE FOR FUTURE WORK

7.1.	CONCLUSION.....	55
7.2.	SUGGESTIONS FOR FUTURE WORK.....	56
	REFERENCES.....	58

LIST OF TABLES

Table	Title	Page
5.1	Specification of testing dataset	25
5.2	Eigen values of first few eigen vectors (TYPE1)	33

LIST OF FIGURES

Figure	Title	Page
3.1	Schematic of a plane parallel medium	11
3.2	Schematic of an isothermal atmosphere model without scattering	12
4.1	Typical simulated radiance of AIRS channels from kCARTA model	18
4.2	Typical simulated brightness temperature of AIRS channels from kCARTA model with the earth's surface temperature as 303.48 K	19
4.3	Flow chart of data processing in kCARTA	19
5.1	Histogram of radiosonde atmospheric profile categorized for various region	22
5.2	Flow chart of synthetic profile generation procedure	23
5.3	Mean / Standard deviation adjusted temperature profile for synthetic profile generation	24
5.4	Mean / Standard deviation adjusted humidity profile for synthetic profile generation	25
5.5	An artificial neural network architecture used for retrieval	28
5.6	Variance contribution of each principal component (TYPE1)	32
5.7	Reconstruction error using principal components (TYPE1)	32
5.8	First three eigen vectors derived from principal component analysis (TYPE1)	34
5.9	First three eigen vectors derived from principal component analysis (TYPE2)	35
6.1	Temperature retrieval performance of PC based linear regression (TYPE1)	38
6.2	Humidity retrieval performance of PC based linear regression (TYPE1)	39

6.3	Humidity retrieval performance of PC based linear regression (TYPE1)	39
6.4	Temperature retrieval performance of PC based ANN (TYPE1)	40
6.5	Humidity retrieval performance of PC based ANN (TYPE1)	41
6.6	Humidity retrieval performance of PC based ANN (TYPE1)	41
6.7	Comparison of PC based linear regression with PC based ANN for temperature retrievals (TYPE1) with (a) 10 (b) 100 and (c) 500 PCs	43
6.8	Comparison of PC based linear regression with PC based ANN for humidity retrievals (TYPE1) with (a) 10 (b) 100 and (c) 500 PCs	44
6.9	Comparison of PC based linear regression with PC based ANN for humidity retrievals (TYPE1) with (a) 10 (b) 100 and (c) 500 PCs	45
6.10	Temperature retrieval performance of PC based linear regression (TYPE2)	46
6.11	Humidity retrieval performance of PC based linear regression (TYPE2)	47
6.12	Humidity retrieval performance of PC based linear regression (TYPE2)	47
6.13	Temperature retrieval performance of PC based ANN (TYPE2)	48
6.14	Humidity retrieval performance of PC based ANN (TYPE2)	49
6.15	Humidity retrieval performance of PC based ANN (TYPE2)	49
6.16	Comparison of PC based linear regression with PC based ANN for temperature retrievals (TYPE2) with (a) 10 (b) 100 and (c) 500 PCs	51
6.17	Comparison of PC based linear regression with PC based ANN for humidity retrievals (TYPE2) with (a) 10 (b) 100 and (c) 500 PCs	52
6.18	Comparison of PC based linear regression with PC based ANN for humidity retrievals (TYPE2) with (a) 10 (b) 100 and (c) 500 PCs	53

NOMENCLATURE

a_{im}	regression coefficient of i^{th} pressure layer and m^{th} term
b	bias of the node
p_l	l^{th} principal coefficient
q	atmospheric humidity, $\frac{g}{Kg}$
s	coordinate along path of radiation, m
	incoming signal to the node
\hat{s}	unit vector in the direction of propagation of the radiation
t	atmospheric parameter measured (K, $\frac{g}{Kg}$)
w	weight of the linkage between nodes
\mathbf{w}	weight matrix of the Artificial Neural Network
y	atmospheric parameter predicted (K, $\frac{g}{Kg}$)
	response of node
z	height from the earth's surface, m
	activation function output
A	design matrix for regression
C	covariance matrix
E	cost function
I	radiative intensity, $\frac{Watt}{m^2 sr^2 cm^{-1}}$
I_β	black body intensity(Planck's Function), $\frac{Watt}{m^2 sr^2 cm^{-1}}$

J	radiosity, $\frac{Watt}{m^2}$
P	matrix of principal coefficients
Q	matrix of eigen vectors
R	matrix of radiances
\hat{R}	matrix of mean subtracted radiances
T	atmospheric temperature, K
Y	matrix of atmospheric parameters

Greek Symbols

β	extinction coefficient, m^{-1}
φ	azimuthal angle, rad
θ	zenith or polar angle, rad
τ	optical coordinate, optical thickness
ω	single scattering albedo
μ	direction cosine of (polar angle) = $\cos \theta$ mean atmospheric profile
η	wavenumber, cm^{-1} randomly generated variable in the range [-3,3]
σ	standard deviation of atmospheric profile
σ_a	linear absorption constant, m^{-1}
σ_s	linear scattering constant, m^{-1}
Ψ	synthetic atmospheric profile
Ω	solid angle, sr

Subscripts

0	at length = 0
i	for i^{th} pressure level
	i^{th} node in previous layer
j	j^{th} node in current layer
L	at height = L, m
nor	normalized
η	at a given wavenumber, cm^{-1}
r	in a given layer

Superscript

'	incoming direction of the radiation
p	for p^{th} step of learning
T	transpose of matrix

CHAPTER ONE

INTRODUCTION

1.1. BACKGROUND

Remote measurements are used for different purposes today, from examining the structure of nucleus to structures of stars, from oil exploration to medical tomography. Whenever direct measurements are difficult or expensive, remote measurements are used, although they often bring with them some complex problems of interpretation, mainly known as inverse problems. Remote measurements are typically necessary for analysis of the earth's atmosphere, wherein inverse methods are required. Much of the conceptual and mathematical approach common to inverse problems cutting across several disciplines has been developed independently using various terminologies. Solving for atmospheric profiles using satellite measured radiances, an inverse problem, is known as remote sounding in parlance of the atmosphere.

A remote measurement is usually one in which the quantity measured is more or less a complicated function of the parameter that is required. The distinguishing characteristic of these measurements is the indirect measurements. Inverse theory refers to the inversion of complicated functions regardless of whether the measurement is physically remote. Typically, in case of say a clear atmosphere, upwelling electromagnetic radiation in the atmosphere is measured by the instrument on satellite and the quantity required is temperature or amount of any constituent of the atmosphere. These satellites offer the advantage of providing us with global data from a single instrument, with excellent spatial coverage.

The inverse problem in question concerns the best representation of required parameter given the measurements made, together with any appropriate prior information that may be available about the system and the measuring device. Remote sounding of the atmosphere has been carried out by a wide variety of instruments, using different principles of measurements. Almost all techniques involve measurement of electromagnetic radiation, although sound propagation has also been used. The physical effects exploited may be refraction, transmittance, scattering, thermal emission and non-thermal emission spanning different wavelengths. Most measurements are passive, measuring naturally generated radiation, but some, notably lidar and GPS are active because they use man-made sources.

1.2. INFRARED SOUNDER

Infrared sounders are devices which measure for the retrieval of temperature and humidity profiles of the atmosphere during non-cloudy conditions, as infrared radiation cannot penetrate clouds. Retrieval of vertical temperature profiles in atmosphere is important for meteorological applications like rainfall rate estimation, determination of geophysical parameters and so on. These are useful not only for short term weather prediction but also for studying climate and its changes over a period of time. Remote sensing of the atmosphere is done using measured infrared radiances. The intensity of radiation leaving the top of the atmosphere, known as TOA radiances depends on the temperature and humidity profiles as well as the concentration of various absorbing gases like ozone and carbon dioxide. For the present work, only high spectral sounders were considered. Given below is a brief description of some well known infrared sounders.

1.2.1. Indian National Satellite System (INSAT 3D)

INSAT-3D is one of three satellites currently being developed by Indian Space Research Organization (ISRO) exclusively to improve domestic weather forecasting and track cyclones and monsoons originating from Bay of Bengal and the Arabian Sea. The instrument comprises a six channel imaging radiometer designed to measure radiant and solar reflected energy from areas sampled on the earth and a 19 channel high resolution infrared sounder to measure vertical temperature profiles, humidity, surface and cloud top temperatures, and ozone distribution. It is planned for launch on the GSLVMk.2 launch vehicle in the year 2010 in a 38,500km equatorial plane geostationary orbit. This orbit will provide a continuous stationary view over the Indian Ocean for regular observations of cloud patterns and monitoring of the path of tropical cyclone formations to predict the time and place of landfall for disaster warning.

1.2.2. Atmospheric Infrared Sounder (AIRS)

AIRS has been in operation since 2002, on board NASA's Aqua Satellite. It provides a spatial resolution of nearly 15km with a spectral resolution of 1200 (i.e. 2378 channels from 650 cm^{-1} – 2675 cm^{-1}). With current remote sensing technology, the AIRS provides a radiometric accuracy of the order of $\pm 0.2\text{ K}$. The Aqua Satellite is deployed in a polar orbit of 700km radius which gives AIRS the capability of scanning almost 90% of the earth's atmosphere (in horizontal dimension) in every 24 hour. This sounder is successfully being used for remote sensing on a global scale.

1.3. MOTIVATION FOR THE PRESENT WORK

The present work involves the development of algorithms for the retrieval of atmospheric temperature and humidity profiles from satellite measured infrared radiances. The algorithms will be useful in selection of channels for a possible hyper spectral sounder mission, that may follow the launch of INSAT 3D. This work is aimed at generating a comprehensive data for the tropical region and developing an effective and robust Principal Component (PC) based algorithm for the retrieval of temperature and humidity, under clear sky condition.

1.4. CLOSURE

In this chapter, the background and motivation for the research work proposed to be undertaken in the present study have been provided. The next chapter presents a review of literature involved during the course of the work.

CHAPTER TWO

LITERATURE REVIEW

2.1. SUMMARY OF LITERATURE REVIEW

Remote sensing of satellite measurements are simply inverse solution to Radiative Transfer Equation (RTE) which mainly deals with estimation of atmospheric properties from known or measured quantities like radiation intensity or brightness temperatures. The algorithms implemented to solve the inverse of RTE are generally categorized as physical retrievals and statistical approaches. The physical retrievals basically work by solving the physics of RTE, an integral-differential equation and validating the solution to satellite measured data. A statistical method, on other hand, derives a mathematical relationship between the measured radiances and the geophysical properties of atmosphere based on previously measured data.

Regardless of its type, the basis of any retrieval algorithm in meteorological application, is the forward model or RTE solutions. Various algorithms like 'line by line' code, fast forward models have been developed to accurately simulate electromagnetic radiances for specified atmospheric conditions. The Atmospheric Infrared Sounder or AIRS fast forward algorithm (*Hannon et al. (1996)*) is one of the advancements made to provide radiances measured by the AIRS in infrared range. In this algorithm, the effective monochromatic layer to space transmittance of the atmosphere is calculated by interpolating among the dataset of specifically chosen 100 atmospheric profile, representing various possible atmospheric conditions. Models like k Compressed

Radiative Transfer Algorithm (kCARTA) (*DeSouza-Machado* (1997)) have also been developed to simulate the infrared radiances using a compressed monochromatic absorption coefficient database. kCARTA, though relatively slow in computation, provides precise infrared radiances when compared with AIRS fast forward model and is therefore, used in this work.

With the cutting edge technology of high resolution measurements from satellites, the volume of data measured has increased tremendously, testing the capacity of current down link technology. The availability of accurate, fast, and easy to use algorithms has become even more important. A major disadvantage with physical retrieval model is the huge amount of computational time taken for processing. The statistical model on the other hand are much faster and efficient in remote sensing and has been implement successfully for Numerical Weather Prediction (NWP).

The use of multilayer feed forward Artificial Neural Network (ANN) for retrieval of atmospheric parameters using hyper spectral measurements was first proposed by *Escobar-Munoz et al.* (1993). Thereafter, many improved retrieval techniques of ANN have been documented using high spectral measurements. The advantage of ANN inversion method is that its provides a model of inverse radiative transfer function, parameterized once and for all conditions, in contrast to classical inversion techniques.

Development of an efficient data compression procedure is crucial for data handling from high spectral resolution measurements and subsequent remote sensing. The application of

Principal Component Analysis (PCA) to the data compression, is one of the advanced statistical methods used in reducing high resolution spectral reading from satellite measurements. *Huang and Antonelli* (2000) have investigated the application of PCA with regression in retrieval of temperature and humidity distribution. Besides obtaining an optimum compression ratio, a desirable subset of principal components (PC) were obtained which gave high retrieval accuracy. They have also discussed the correlation between the PCs and the atmospheric temperature / humidity distribution and noise removal from the spectral data achieved by PCA.

Combining both the ANN model with PCA gives an enhanced performance of remote sensing. *Aires¹ et al.* (2002) applied the concept of PCs for compressing, denoising and first guess retrieval from the reading of Infrared Atmospheric Sounding Interferometer (IASI), a high resolution sounder. This analysis used 8461 channel of IASI as against 2378 channels of AIRS. The first guess retrieval was then applied to a PC based ANN (*Aires² et al.* (2002)) to retrieve simultaneously the temperature, water vapor and ozone profile. The result obtained showed an overall improvement in accuracy of the retrievals using ANN.

An advanced version of PCA, known as Projected PC Transform (PPC) was used by *Blackwell* (2005) along with ANN for retrieval purposes. The performance of PPC based ANN algorithm in retrieving temperature / humidity profiles was very good when compared with PPC regression and Iterated Minimum Variance Techniques (IMV).

The above literature review shows that retrieval of vertical atmospheric profiles from observed infrared radiances has been done by various techniques ranging from statistical to non-linear physical methods. Uncertainty in the retrievals is more pronounced for the humidity profile than for the temperature profile. In the present work, only clear sky situations were taken into account. Increase in number of spectral channels brings in the problem of channel selection too, but reduces the ill-posed nature of the retrieval. The inverse problem dealing with the retrieval of vertical atmospheric profiles from the observed infrared satellite radiances needs a retrieval algorithm that is robust so that real time retrievals can be performed with less uncertainty, whenever they are required.

The present work aims at studying the performance of PC based ANN algorithm in retrieving the temperature / humidity profile using high spectral resolution measurements. PC based regression algorithms is also developed for the retrieval and its performance is compared with PC based ANN algorithms. The algorithms are trained using mixed sets of synthetic and realistic profiles and the retrieval accuracies are tested extensively for both synthetic and realistic profile independently.

2.2. CLOSURE

A general survey of pertinent literature for the retrieval of temperature / humidity profile was presented in this chapter. The objectives and scope of the present investigation were also clearly described. The next chapter presents the mathematical formulation and the methodology adopted in the present work.

CHAPTER THREE

MATHEMATICAL FORMULATION

3.1. INTRODUCTION

Radiative Transfer Equation (RTE) is the basic equation in remote sensing of atmospheric profiles. Various forward / fast forward model have been developed on this equation. RTE explains the propagation of electromagnetic radiation through an absorbing, emitting and scattering medium. In particular, it is the integral differential nature of the equation, which make it complex for computations. In this present work, the propagation of electromagnetic radiation in infrared spectral range is considered. As clouds are opaque to infrared radiation, non cloudy conditions of the earth's atmosphere are considered and hence the contribution of scattering is neglected in the radiative transfer equation.

3.2. RADIATIVE TRANSFER EQUATION

3.2.1. One Dimensional Radiative Transfer Equation

A gaseous medium is said to be 'participating' when any incident beam is attenuated by absorption or scattering within the medium. In the present case, the earth's atmosphere is considered as a participating medium through which long wave upwelling radiation from the earth's surface, passes and gets attenuated by absorption from various gases present. The absorption spectra are then recorded at the top of the atmosphere from infrared sounders.

In general, the amount of absorption dI_η , in η spectral line, within a participating medium has been observed to be directly proportional to the magnitude of incident energy I_η as well as to the distance traveled along the medium s , $(dI_\eta)_{abs} = -\sigma_{a\eta}I_\eta ds$. The proportionality constant is known as the linear absorption constant $\sigma_{a\eta}$. Similarly, scattering attenuation, in scattering augmentation and emission augmentation of the beam takes place within the participating medium, which can be summed up into a complex integro-differential equation

$$\frac{dI_\eta}{ds} = -(\sigma_{a\eta} + \sigma_{s\eta})I_\eta + \sigma_{a\eta}I_{\beta\eta} + \frac{\sigma_{s\eta}}{4\pi} \int_{4\pi} I_\eta(\hat{s}') \Phi_\eta(\hat{s}', \hat{s}) d\Omega' \quad (3.1)$$

The spectral intensity I_η is a function of the space coordinates s and angular coordinates φ , θ and $I_{\beta\eta}$ is the spectral black body intensity derived from the Planck's black body function. The RTE equation 3.1 is usually solved in the non dimensional form

$$\frac{dI_\eta}{d\tau} = -I_\eta + (1 - \omega_\eta)I_{\beta\eta} + \frac{\omega_\eta}{4\pi} \int_{4\pi} I_\eta(\hat{s}') \Phi_\eta(\hat{s}', \hat{s}) d\Omega' \quad (3.2)$$

in terms of optical depths τ_η and single scattering albedo ω_η defined by

$$\omega_\eta = \frac{\sigma_{s\eta}}{(\sigma_{a\eta} + \sigma_{s\eta})} = \frac{\sigma_{s\eta}}{\beta_\eta} \quad (3.3)$$

$$\tau_\eta = \int_0^s (\sigma_{a\eta} + \sigma_{s\eta}) ds = \int_0^s \beta_\eta ds \quad (3.4)$$

This equation represents radiation propagation in one dimensional participating medium. Certain assumptions were made to make this equation compatible for propagation in the atmosphere of infrared waves, which are discussed in the subsequent section.

3.2.2. Plane Parallel Medium Assumption

The height of the earth's atmosphere scales up to an order of 10^2 km and with high resolution viewing of current infrared sounders (13 km at nadir of Atmospheric Infrared Sounder (AIRS)), the plane parallel medium approximation is sufficient in calculating the infrared absorption spectrum of the atmosphere accurately. Under this assumption, the earth's atmosphere is partitioned into various plane parallel layers with different values of layer averaged atmospheric parameters.

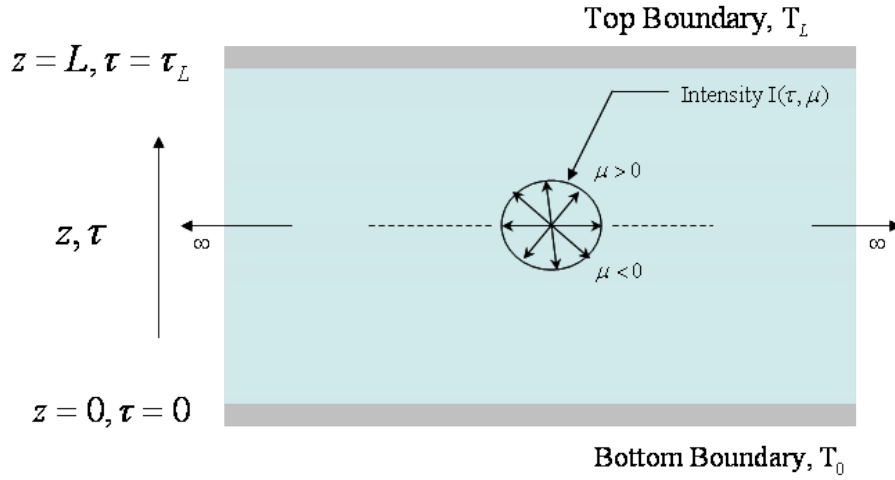


FIGURE 3.1: Schematic of a plane parallel medium

FIGURE 3.1 shows a one dimensional homogeneous participating medium of thickness L bounded by two parallel surfaces at different temperatures. The atmosphere can be modeled in a similar way with the vertical atmosphere being divided into a finite number of layers. The gas volumes are sparse at higher altitudes and so it is a common practice to make finer layers near the earth's surface and wane the layer thickness with increasing height from the earth's surface.

As we are concerned with wave number in the range of infrared spectrum, the scattering term in RTE can be neglected. Infrared sounding is used only in non-cloudy conditions as

clouds are opaque to infrared radiation. In the case of radiation in infrared range, RTE simplifies to

$$\mu \frac{dI_\eta(\tau, \mu)}{d\tau} = -I_\eta(\tau, \mu) + (1 - \omega)I_\beta \quad (3.5)$$

where $\mu = \cos\theta$ is the factor which takes care of the direction of propagation of long waves with θ as the view angle of the sounder from nadir. For the present analysis, $\theta = 0$ as the AIRS sounder is in nadir orientation when sensing infrared radiances.

The forward problem under consideration here is the equation 3.5 for a given set of radiative properties. The solution of equation 3.5 gives us the radiances or intensities at the top of the atmosphere. In the case of atmospheric remote sensing, the atmosphere is modeled as a non-gray participating medium made up of a number of isothermal plane parallel layers, with each layer having different absorption and emission coefficients.

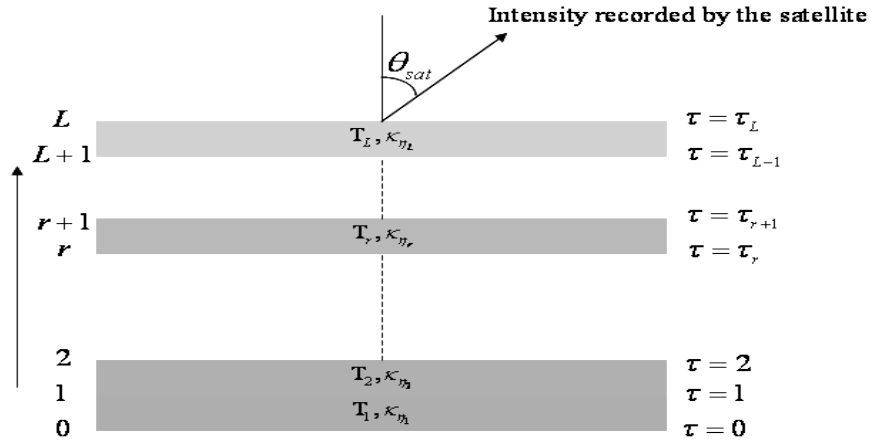


FIGURE 3.2 : Schematic of an isothermal atmosphere model without scattering

Equation 3.5 is a simple first order ordinary differential equation. This can be solved by exact methods. The bottom surface is assumed to be a diffusely emitting and reflecting surface. The solution of equation 3.5 for any layer in the atmosphere in case of upwelling radiation from the earth's surface is given as

$$I_{\eta r}(\tau, \mu) = I_{\eta}(\tau_r, \mu) e^{\frac{-\tau}{\mu}} + I_{B\eta}(T_r)(1 - e^{\frac{-\tau}{\mu}}), \quad \mu > 0, \quad r=1,2,\dots,L \quad (3.6)$$

$$I_{\eta r}(\tau, -\mu) = I_{\eta}(\tau_{r+1}, -\mu) e^{\frac{-(\tau-\tau_L)}{\mu}} + I_{B\eta}(T_r)(1 - e^{\frac{-(\tau-\tau_L)}{\mu}}), \quad \mu > 0, \quad r=1,2,\dots,L \quad (3.7)$$

The upwelling intensity at the bottom surface can be obtained from radiosity of the surface and the corresponding expression is given by

$$I_{\eta}(0, +\mu) = \frac{J_{\eta}(0)}{\pi} = \varepsilon_0 I_{B\eta}(T_0) + 2(1 - \varepsilon_0) \int_{\mu=-1}^0 I_{\eta}(0, -\mu) d\mu, \quad \mu > 0 \quad (3.9)$$

T_0 is the bottom surface temperature and ε_0 stands for emissivity at the surface. From equation 3.7, it is clear that the upwelling intensity at the bottom surface is a function of downwelling intensity. As we know the downwelling intensity at the top of the atmosphere, final solution for the upwelling intensity at top of the atmosphere can be obtained as follows:

- 1) The integral in equation 3.9 is replaced by summation over that range using a suitable quadrature scheme.
- 2) Solve for the downwelling intensities at each quadrature point in each layer by marching downwards (equation 3.7) from the top layer and finally determine the downwelling intensities at the bottom surface.
- 3) Now calculate the upwelling intensity in μ_{sat} ($= \cos\theta_{\text{sat}}$) direction from equation 3.6 and the obtained downwelling intensities.
- 4) Calculate the upwelling intensity in μ_{sat} direction for each layer by marching upwards (equation 3.6) from the bottom layer and determine the upwelling intensity at top of the atmosphere in the viewing direction of the satellite.

An exact solution is possible for the solution of RTE under clear sky conditions. Optical thicknesses of different layers and absorptivity of various gases at different frequencies need to be known accurately for the solution of RTE. In this work kCompressed Atmospheric Radiative Transfer Algorithm (kCARTA, *De Souza-Machado et al. (1997)*) was used for the solution of the RTE and will be discussed in detail in the next chapter.

3.3. METHODOLOGY

The solution methodology adopted in this study essentially aims at formulating the retrieval of atmospheric profiles as an optimization problem. This is achieved by using a forward model, which gives output radiances in different channels of AIRS for a given atmospheric profile input. These high spectral radiances are reduced in dimensionality and retrieved using statistical tools. This model is then trained using the reduced inputs and tested with both synthetic and realistic profiles. This procedure is repeated for various reduction in data and the optimum compression is evaluated based on the retrieval performance. The present study uses two retrieval model: linear regression and Artificial Neural Network (ANN) and a data compression techniques, Principal Component Analysis (PCA). The objective of the study is to evaluate the application of PCA in retrieval problems and compare the performance of PC based regression with PC based ANN.

3.4. CLOSURE

The mathematical formulation adopted in this study was elucidated in this chapter. The RTE with plane parallel modeling of the atmosphere was discussed and solved for 'no

scattering' conditions in the earth's atmosphere. A brief description of the methodology followed in this analysis has also been presented in this chapter. The methodology has been discussed in detail in CHAPTER FOUR and CHAPTER FIVE and the results of the present study have been discussed in CHAPTER SIX.

CHAPTER FOUR

FAST FOWARD MODEL

4.1. k COMPRESSED RADIATIVE TRANSFER ALGORITHM (kCARTA)

4.1.1. Introduction

Line by line radiative transfer models are very essential in the retrieval of atmospheric parameter using satellite measurements. These models performs the computation of monochromatic layer transmittance for a specified atmospheric condition, which are further evaluated to compute spectral radiances. They effectively utilize the physics of radiative transfer for a participating medium and successively calculate physical attributes for each spectral line i.e. by 'line by line' radiative transfer. The current state of the art in infrared sounders are high spectral resolution sensors (0.25cm^{-1} for Infrared Atmospheric Sounding Interferometer (IASI) and 0.50 cm^{-1} for Atmospheric Infrared Sounder (AIRS)), which are testing the accuracy of established line by line models. At the same time, computing budget of these models has increased, leading to the development of fast algorithms in radiative transfer.

For the purpose of speeding up the computation, the AIRS fast forward transmittance model (*Hannon et al. (1996)*) was developed. In this model, the monochromatic layer to space transmittance were accurately calculated for more than 100 atmospheric profiles, chosen to cover a wide range of temperature and humidity variation. These transmittances were then convolved with spectral response functions of the sounder to produce effective layer transmittances which were parameterized as functions of atmospheric variables.

Another method of improving the radiance transfer model was to use a compressed database of atmospheric absorption coefficient as applied in the kCARTA model. kCARTA, though slower in computation than the AIRS fast forward model, results in accurate radiance data as that of line by line models, thereby an appropriate choice for simulating radiances in the present work.

4.1.2. Features of kCARTA

kCARTA is an infrared, monochromatic radiative transfer algorithms used for a one dimensional non scattering earth's atmosphere. The radiance simulated in present work are pertaining to nadir viewing of the AIRS on board NASA's Aqua Satellite. In the working of kCARTA, only the basic version of the model is used to handle clear sky radiative transfer computation, with no radiative scattering. An emissivity dataset is also included in the algorithm to represent the surface and layer emission terms.

The radiative transfer equation solved by the model uses absorption coefficients computed by k-compressed lookup tables, compressed using singular value decomposition techniques (*Strow, L. L. et al. (1996)*). These absorption coefficients are strongly dependent on absorbing gas amount and shows a slow variation with temperature. Therefore, the absorption coefficients are computed by interpolated with respect to the temperature within the k-compressed database for any arbitrary atmospheric profile. These coefficients are then used in the radiative transfer equation to give accurate radiances in the infrared region of electromagnetic wave.

FIGURE 4.1 and FIGURE 4.2 depicts the radiances simulated by kCARTA for a specified atmospheric condition. Shown are the radiance readings in the infrared spectrum corresponding to the 2378 channels of AIRS. The overall coverage of the sounder lies between 650cm^{-1} to 2700cm^{-1} , and therefore has the capability to capture the absorption behavior of almost all constituents of the atmosphere.

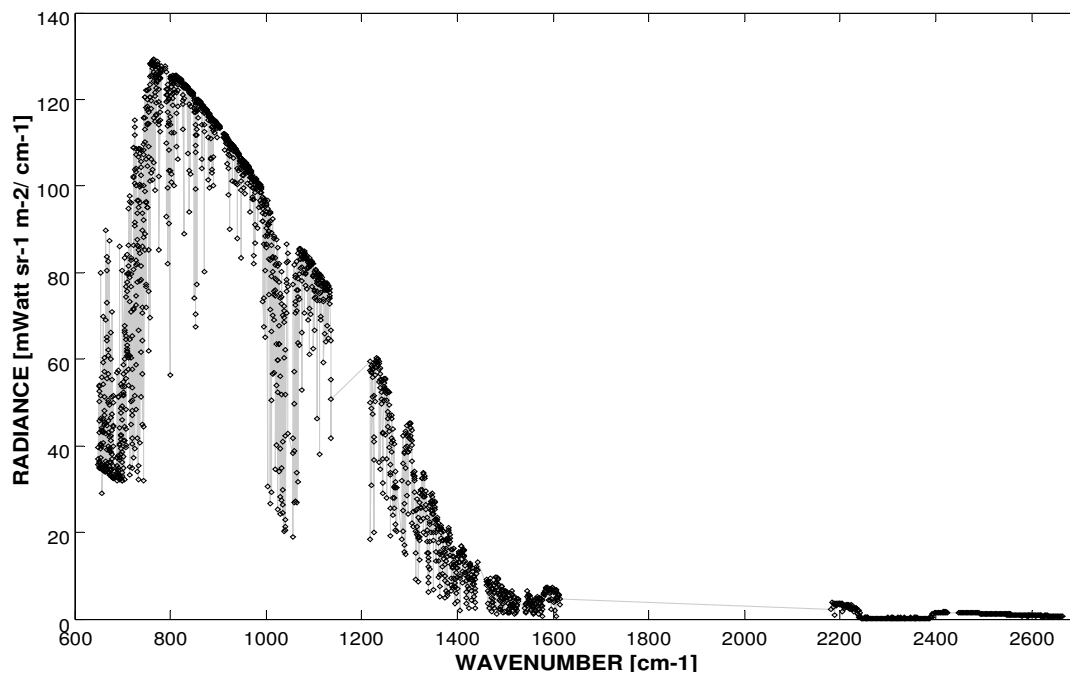


FIGURE 4.1 : Typical simulated radiance of AIRS channels from kCARTA model

The flow chart in FIGURE 4.3 shows the operation of kCARTA through various processing stages. The input profile is first processed through kLAYER, a function which converts point profiles to layer averaged temperature profile. kLAYER routine convert the atmospheric profile to the Radiative Transfer Profile (RTP) format which is compatible with kCARTA program. This RTP file along with namelist containing the wavenumber range and the emissivity information is fed into the main program of kCARTA which gives the radiances in infrared region as specified.

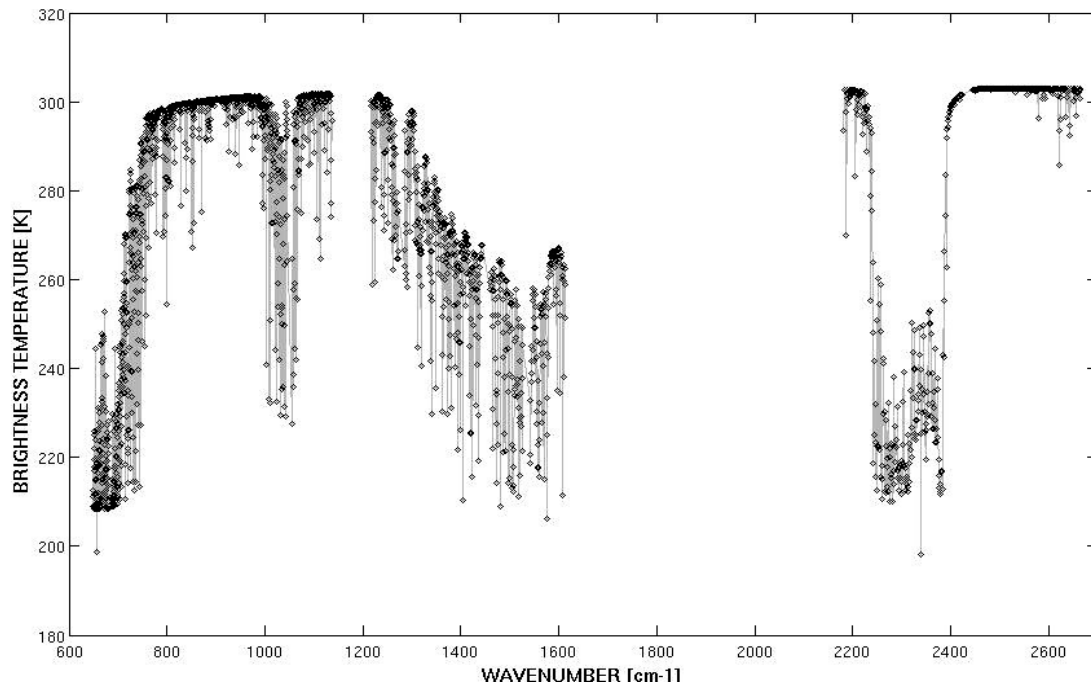


FIGURE 4.2 : Typical simulated brightness temperature of AIRS channels from kCARTA model with the earth's surface temperature as 303.5 K

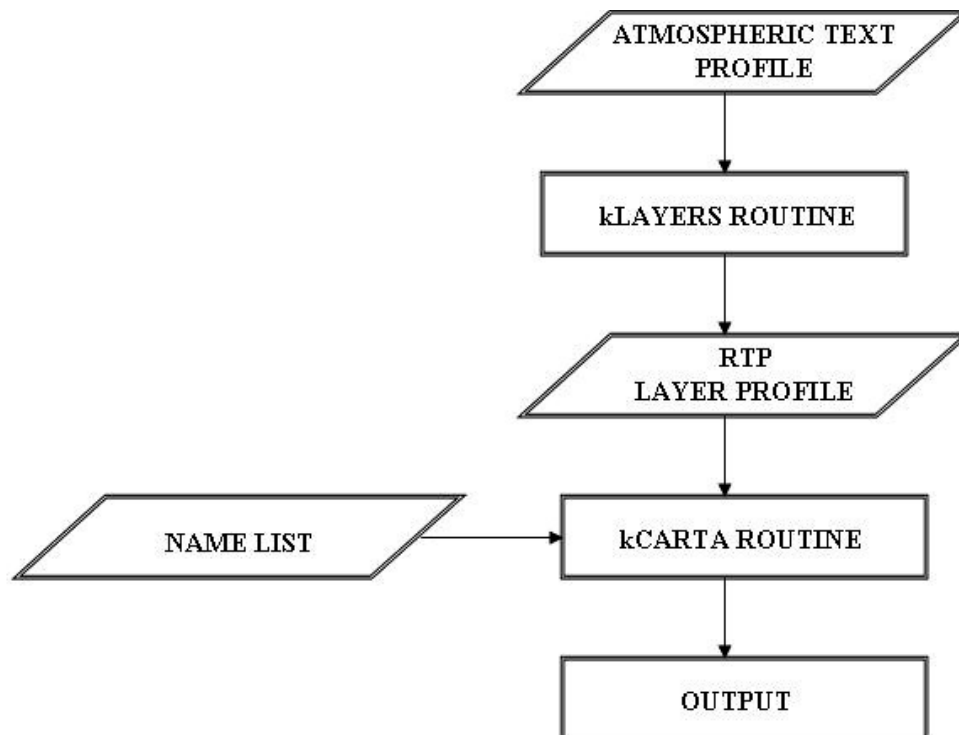


FIGURE 4.3 : Flow chart of data processing in kCARTA

4.2. CLOSURE

A detailed explanation of the working of fast forward model kCARTA is provided in this chapter. The pertinent features of kCARTA are also explained briefly. The following chapter presents the application of statistical methods in temperature / humidity retrievals of the atmosphere.

CHAPTER FIVE

RETRIEVAL ALGORITHMS

5.1. DATABASE FOR RETRIEVAL ALGORITHM

5.1.1. Realistic Dataset

Realistic datasets in a statistical problem solving method, always holds the key to robustness of the algorithm. These profiles determine the accuracy and efficiency of the retrieval, as most of the statistical tool functions by interpolating among these datasets. With this emphasis, a large set of reliable and authentic atmospheric profiles have been used in computations.

A typical database profile includes the distribution of temperature, density, water vapor and ozone gas along pressure levels ranging from standard surface pressure (1013 millibars) to highest layer pressure. While kCARTA utilizes all parameters in these profiles, it uses standardized quantity of minor gases present in the atmosphere, producing realistic upwelling infrared radiances emitted at the top of the earth's atmosphere. This combination of the atmospheric profiles with their corresponding infrared signatures is used in training, validation and testing of the retrieval algorithm.

The ground truth for these studies were the radiosonde profile available from many sources (FIGURE 5.1) . The available profiles were classified into three categories: (1) Tropical Region Profiles (2) Temperate Region Profiles and (3) Polar Region Profiles. Only the Tropical Region Profiles were used in all computations of the present work.

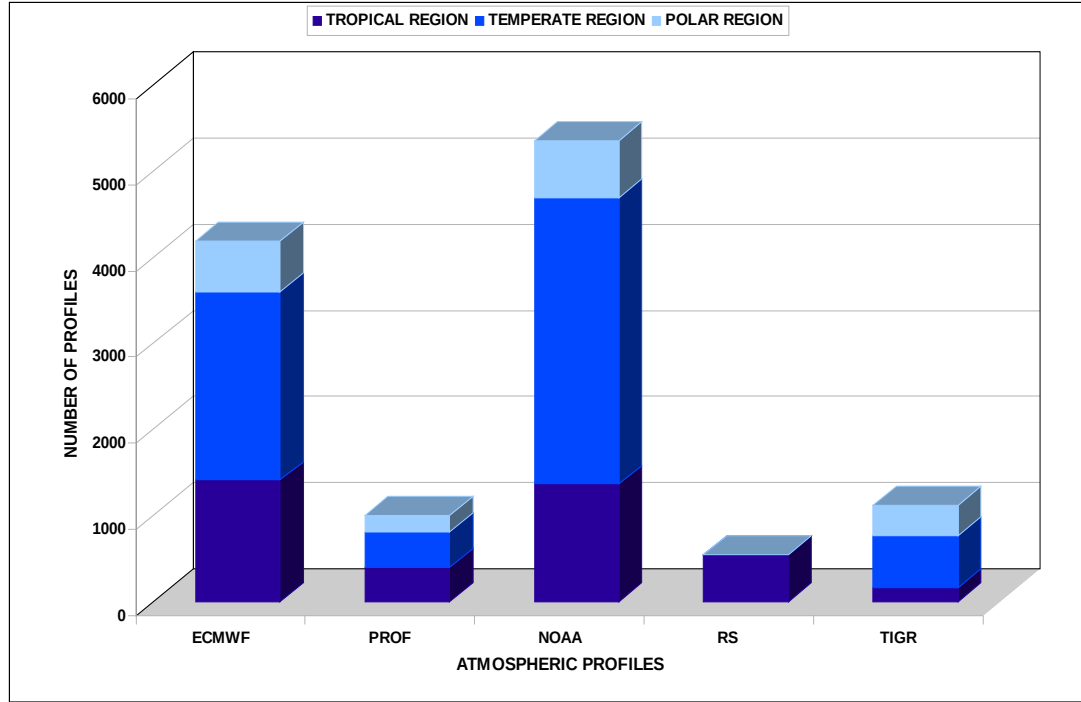


FIGURE 5.1 : Histogram of radiosonde atmospheric profile categorized for various region

5.1.2. Synthetic Profiles

For retrieval purposes, it is imperative that the datasets used for determining the relationship between the input and output are reliable. It is also important that these datasets contains large enough profiles to improve generalization of the algorithm. With sufficient number of realistic profile available, it is possible to generate various atmospheric profiles feasible in nature. Having a limited availability of realistic profile (3900 tropical profiles), synthetically created profiles (around 7000) were included in training datasets. This gives an added advantage of including those atmospheric conditions which were not featured in the realistic profiles.

A simple criterion has been used to generate the synthetic profiles required for training the neural network architecture used for retrieval purpose. FIGURE 5.2 shows all the

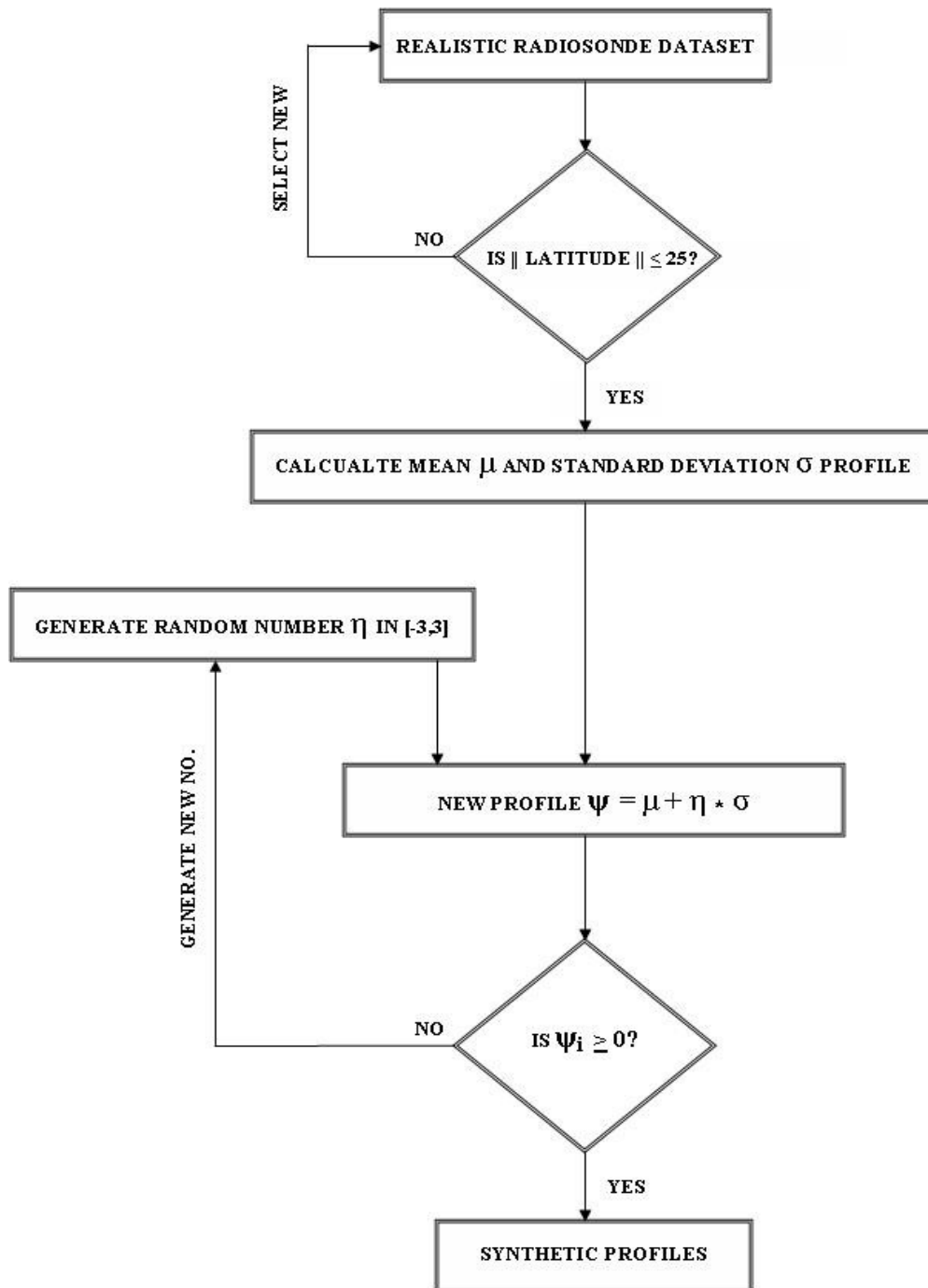


FIGURE 5.2 : Flow chart of synthetic profile generation procedure

stages of procedure required for making synthetic profiles. The mean distribution μ and the RMS variation σ of atmospheric parameters (temperature, density, water vapor and ozone) are calculated for the 3900 tropical profiles. Assuming that each parameter

follows a gaussian distribution about its mean, the synthetic profile of parameters are calculated by generating values varying between $\mu - 3\sigma$ to $\mu + 3\sigma$, giving a 99.997% probability of occurrence in nature. The new profile Ψ is generated using the equation $\Psi = \mu + \eta\sigma$, where η is a random number in the range $[-3,3]$. To ensure smoothness of the profiles, only a single random number is used for each profile generation. By applying the criterion of non negative values for Ψ , its ensured that the parametric values are physically realistic. FIGURE 5.3 and FIGURE 5.4 shows the domain for creating the synthetic profile. The averaged variation of temperature / humidity profile is also shown in the figures for all pressure levels.

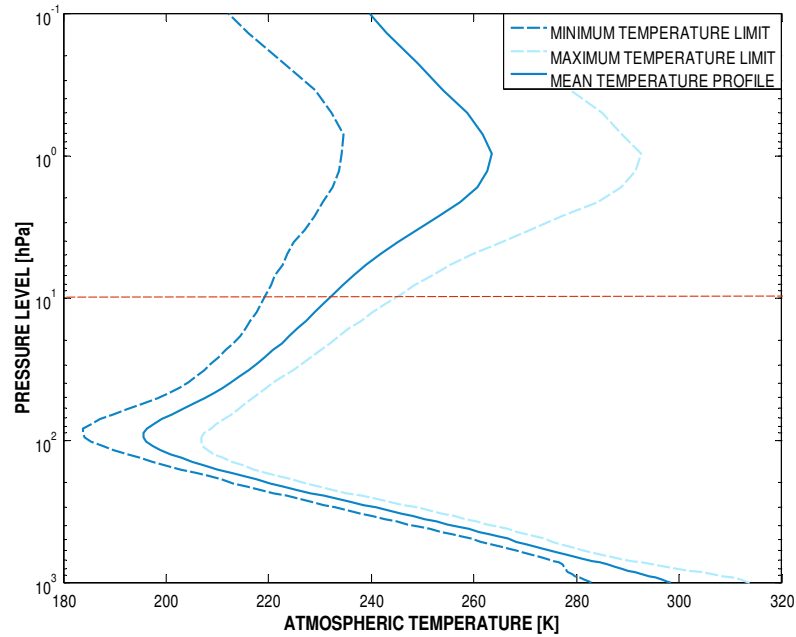


FIGURE 5.3 : Mean / Standard Deviation adjusted temperature profile for synthetic profile generation

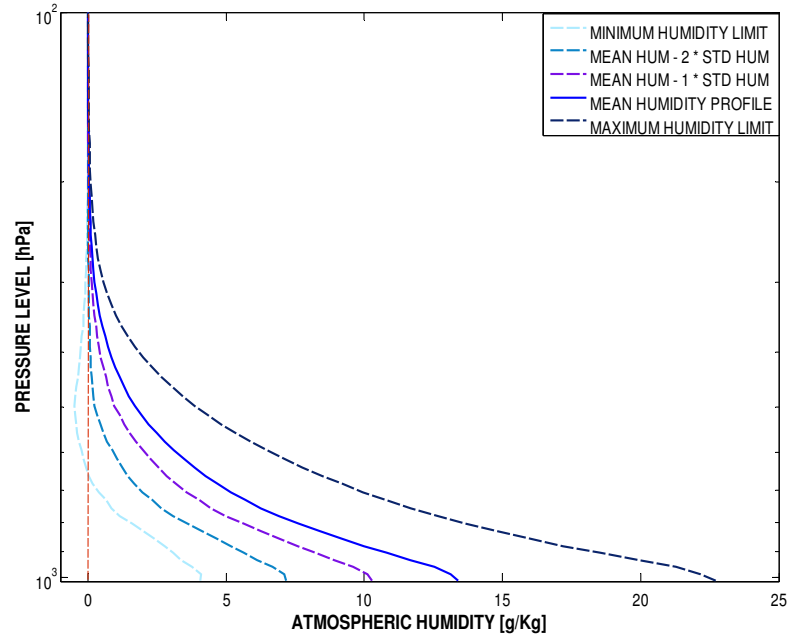


FIGURE 5.4 : Mean / Standard deviation adjusted humidity profile for synthetic profile generation

5.1.3. Training and Testing Datasets

For better retrieval performance of the statistical models, a mixed dataset of 3500 realistic profiles and 7000 synthetic profiles was used for determining the relationship between principal components and their corresponding temperature / humidity profile. Testing the generalization of the statistical model were two datasets TYPE1 and TYPE2, which are shown in the TABLE 5.1 .

TABLE 5.1 : Specification of testing dataset

DATASET	PROFILES
TYPE1	Synthetic Profile (3000)
TYPE2	RadioSonde (RS) Profile (540)

5.2. REGRESSION

Regression methods were the first retrieval algorithms used in sounding techniques. They are statistical or non-physical retrieval methods because they do not explicitly make use of the radiative transfer physics in computation. The advantage of such methods is that they are used independent of any radiative transfer model, which makes their performance much faster and efficient. Measured radiance data can be colocated with radiosonde measurements to build sets of training data directly (Xuebao *et al.* (2005)).

A linear additive (hyperplane) model is used in the regression of the atmospheric parameters y_i of i^{th} pressure level, with $y_i = a_{i0} + a_{i1}p_1 + a_{i2}p_2 + a_{i3}p_3 + a_{i4}p_4 + \dots + a_{ik}p_k$ where p_l ($l = 1, 2, \dots, k$), a_{im} ($m = 0, 2, \dots, k$) are the chosen k principal components or predictor variable with their respective regression coefficients. With n readings, the equation becomes a matrix equation of the form $[Y] = [A][P]$, $[Y]_{p \times n}$ being the matrix of atmospheric parameters having temperature and humidity profiles arranged in columns, $[A]_{p \times (k+1)}$ being the matrix of regression coefficients arranged in rows for each parameter y_i and principal components matrix $[P]_{(k+1) \times n}$ with the components arranged in column and $p_0 = 1$ for all columns. The regression coefficients are calculated for the training sets, validated with the testing sets and the cost function E is evaluated to record the performance of the regression for each layer i.e.

$$E_i = \left(\sum_{l=1}^N (t_{li} - y_{li})^2 \right)^{1/2} \quad (5.1)$$

where t_i of i^{th} pressure level is target value of the parameter.

The use of principal components as predictor vectors gives a large compression of radiance data and makes the regression more stable. Reduction of principal components becomes more relevant when number of channels involved is quite high, as in with the Atmospheric Infrared Sounder(AIRS) radiance data of 2378 channels used in present work.

The linear additive model used here is a basic regression model, which could be improved by applying complex regression methods. However, in general, linear regression forms a sort of benchmark against which retrieval by other methods like ANN can be compared.

5.3. ARTIFICIAL NEURAL NETWORK (ANN)

The architecture of any neural network comprises of an interconnection of basic processing units or nodes. The connectivity within the network is such that, each node receives a weighted sum of responses from nodes present in previous layer. To create a following response, the incoming signal is processed by an activation function, with adjustments to the signal by adding a bias. A response when generated by the node is passed on to next nodes through connectivity, thereby repeating the same process till final output is reached at the outer layer (FIGURE 5.5) .

These activation function, linear or non-linear in nature, are the most integral part of neural network, as they determine the learning performance of the whole architecture. Most commonly used activation functions are linear, sigmoid, hyperbolic tangent

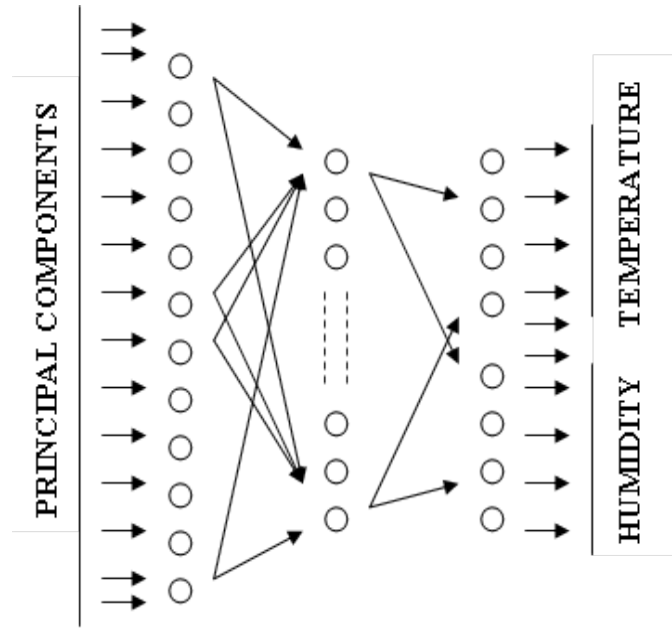


FIGURE 5.5 : An artificial neural network architecture used for retrieval

and radial basis functions. The added advantage of ANN is its learning ability i.e. to deduce an input-output relationships from a training ensemble irrespective of the distribution of data.

There is no established method to determine the optimum number of hidden layers or the number of neurons in each layer and so they have to be determined iteratively. When there are too few neurons in the layers, a large bias exist between the output and target. Too many neurons in network leads to problem of over fitting, where the network is over-trained by training ensemble but performs badly when tested for generalization. Therefore, an optimal network is determined heuristically by operating for various configurations. Convergence of the output and computation time are also some attributes which are considered when evaluating the network.

For the present work, the neural network toolbox of MATLAB7.0 (*Demuth (2009)*) was used. A feed forward back propagation neural network was chosen for an input layer of principal components with an output layer consisting of normalized temperature and water vapor content and no hidden layers. The first 96 outputs nodes of temperature were normalized by $T_{\text{nor}} = 300 \text{ K}$ while the water vapor content in the output were normalized by $q_{\text{nor}} = 15 \text{ g/Kg}$. The output layer contains the linear activation function of the form $z_j = s_j$, where $s_j = \sum_i w_{ji} y_i + b_j$ and y_i is a response by i^{th} node in previous layer. The weights w_{ji} connecting i^{th} node with j^{th} node and bias b_j are iteratively calculated by the back propagation learning method. TRAINSCG routine or scaled conjugate gradient method was typically used for the training, which can handle a large dataset (10000 to 12000 sets of input / output combination). TRAINSCG routine uses the conjugate gradient search method, where the search direction is determined conjugate to the previous search direction (i.e. to combine new steepest descent direction with the previous search directions), along with the model-trust region approach (used in the Levenberg-Marquardt algorithm).

The overall performance of a trained ANN is given by the cost function defined in equation 5.1 . For analyzing training performance of an ANN, for a set of weights and bias \mathbf{w} , a cost function is chosen $E(\mathbf{w})$ such that

$$E^p(\mathbf{w}) = \frac{1}{2} \sum_k (t_k^{(p)} - z_k^{(p)})^2 \quad (5.2)$$

where $t_k^{(p)}$ and $z_k^{(p)}$ denotes the network target and output, respectively, of each output node k given at p^{th} iterative step of learning. Most of the back propagation algorithms

uses this parameter explicitly to update weights / bias of the network. As many as, 10000 epochs or generation were used for each case to ensure adequate training of the network and sufficient convergence of solution. The results of the ANN retrieval are discussed in the next chapter.

5.4. PRINCIPAL COMPONENT ANALYSIS (PCA)

With the advent of modern atmospheric sounders, there has been a growing demand for more robust and accurate weather prediction models. It is imperative that retrieval procedures involve maximal usage of geophysical content of hyper spectral radiance data for its prediction. Principal Component Analysis or PCA is one of the powerful statistical tools which is utilized for improving data usage. It involves categorizing data on the basis of their covariance with each other and effectively reduces the data dimensionality by discarding less relevant dimensions. Besides being a valuable tool for compressing spectral data, PCA is also used for smoothening instrument noise that is contained in radiance measurements by neglecting higher order variances.

In the computation, a single infrared reading from the AIRS channels was considered as a radiance vector $\{R\}$ in m -dimensional subspace ($m = 2378$). With p readings from the AIRS channels, the radiance vector was arranged column wise in a matrix $[R]_{m \times n}$ of $m \times n$ dimensions. If Q_k^T is the PC operator, a linear, orthonormal operator which projects a m -dimensional radiance vector into an k -dimensional ($k \leq m$) subspace then principal components $[P]_{k \times n}$ of the radiances are $[P] = Q_k^T[\acute{R}]$. $[\acute{R}] = [R] - R_\mu$ are reduced radiances with R_μ mean of radiance vector subtracted from each observation. The rows

of Q_k^T contains the k most significant eigenvectors (sorted by descending eigenvalues) of data covariance matrix C_{RR} , where $C_{RR} = \langle \dot{R} \cdot \dot{R} \rangle$.

The evaluation of PCA retrievals were done on the basis of two important outcomes;

(i) accuracy of prediction in terms of mean RMS error, which should be within the standards set by World Meteorological Organization (i.e. within 1K for temperature retrieval and 20-30% relative error for humidity retrieval) and (ii) best compression or component reduction possible to maintain the accuracy limits.

Each eigen vector of the covariance matrix C_{RR} represents a unique, linear and orthogonal variance contributor to the dataset. Projecting each radiance observation onto the eigen vector, will capture the variance feature represented by this vector. By ordering the vectors on the basis of their eigen values, we intend to classify the variance features of the data. FIGURE 5.6 shows the contributions of principal components starting from most prominent component for a typical dataset (TYPE1). As depicted, the eigen values decreases exponentially, thereby limiting important features to only first few components. Another way of depicting the contribution of various components is by reconstructing the original data using first few principal components. The reconstructed data $[\dot{R}_R] = Q_k Q_k^T [\dot{R}]$ is obtained by the operator $Q_k Q_k^T$; comparison with the original data $[\dot{R}]$ will show an error deviation. FIGURE 5.7 shows that even by using a minimum of 100 components, the reconstruction error reduces to less than $10 \text{ mWatt m}^{-2} \text{ sr}^{-1} / \text{cm}^{-1}$.

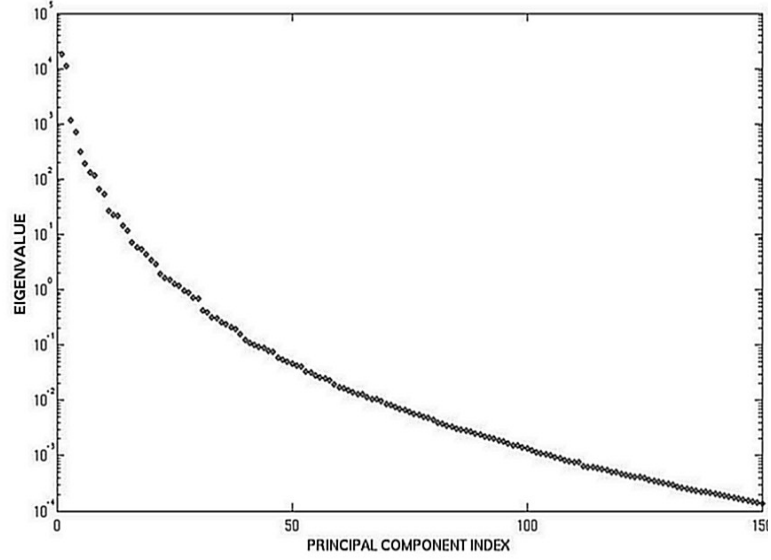


FIGURE 5.6 : Variance contribution of each principal component (TYPE1)

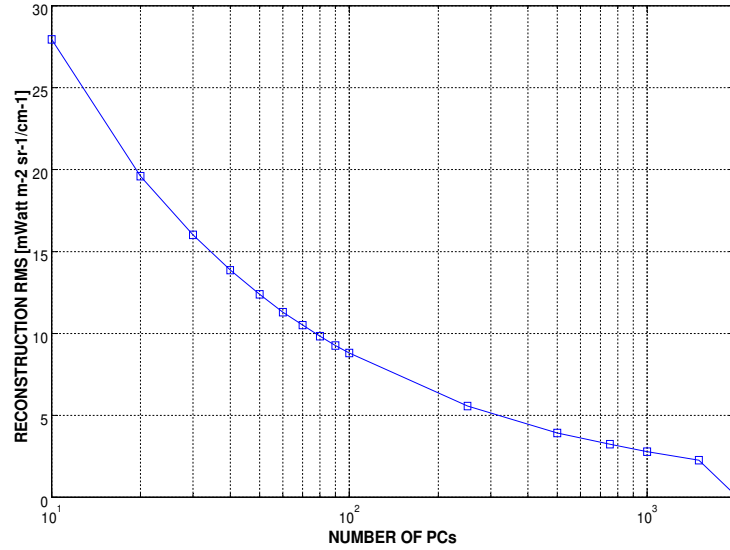


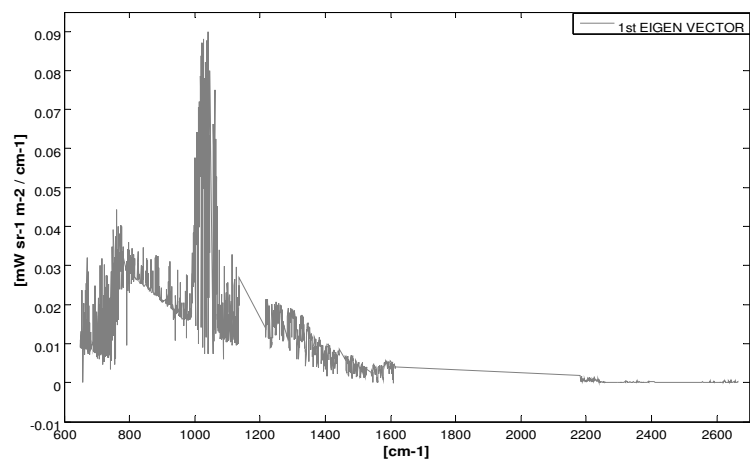
FIGURE 5.7 : Reconstruction error using principal components (TYPE1)

TABLE 5.2 shows typical eigen values of prominent vectors along with their cumulative contributions in variance. The first three eigen vector account to 95% variance contribution in dataset TYPE1 which makes them the most important features of the dataset. Yet, in the retrieval method an average of 100 to 300 principal components are used for the most optimal prediction (*Huang (2001)*) and up to 500 principal

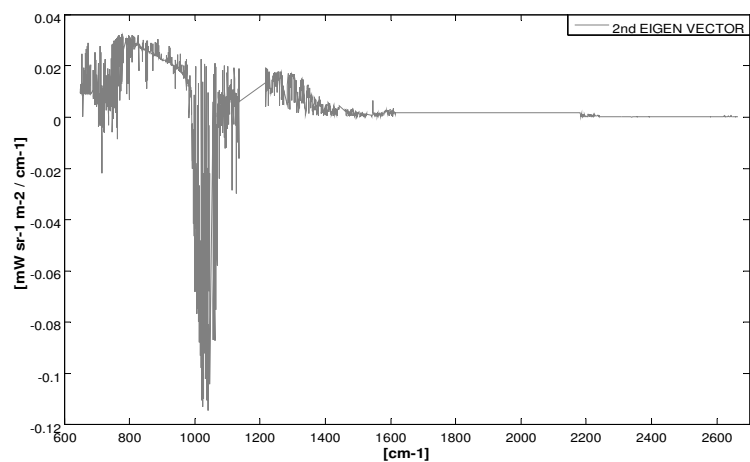
components are used for noisy radiances dataset (*Blackwell* (2005)). Shown in FIGURE 5.8, 5.9 are the first three prominent eigen vectors in TYPE1 and TYPE2 dataset respectively.

TABLE 5.2 : Eigen values of first few eigen vectors (TYPE1)

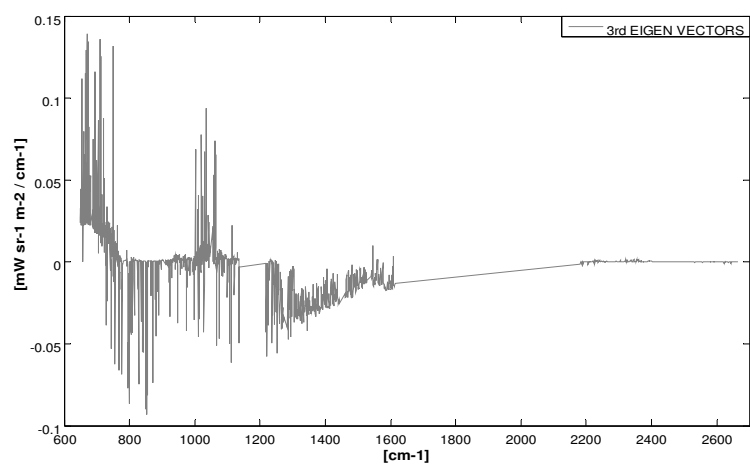
PRINCIPAL INDEX	EIGEN VALUE	CUMULATIVE %
1	17993.3093	56.2658
2	11087.8259	90.9379
3	1185.3443	94.6446
4	699.7194	96.8326
5	315.0443	97.8178
6	188.2016	98.4063
7	130.9496	98.8158
8	117.8997	99.1844
9	65.0963	99.3880
10	54.6386	99.5589



(a)

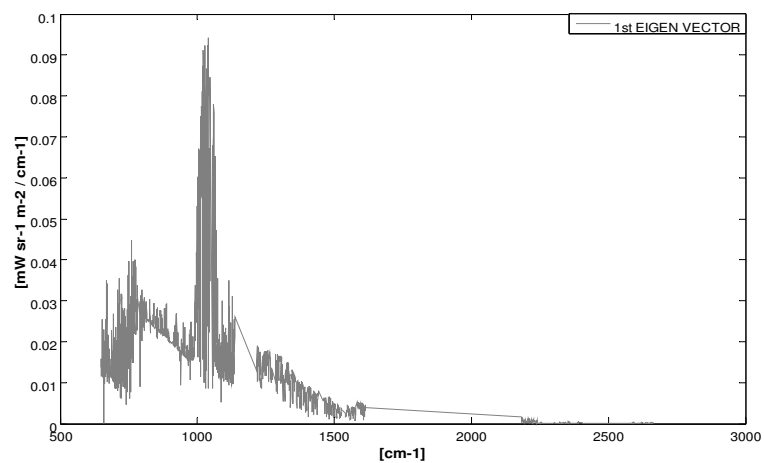


(b)

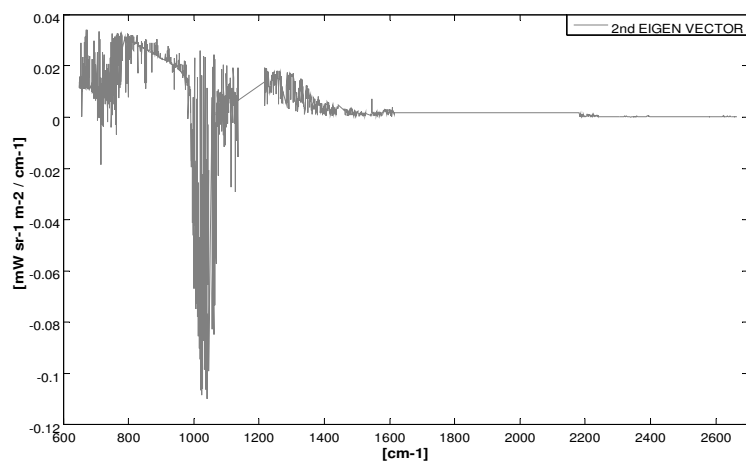


(c)

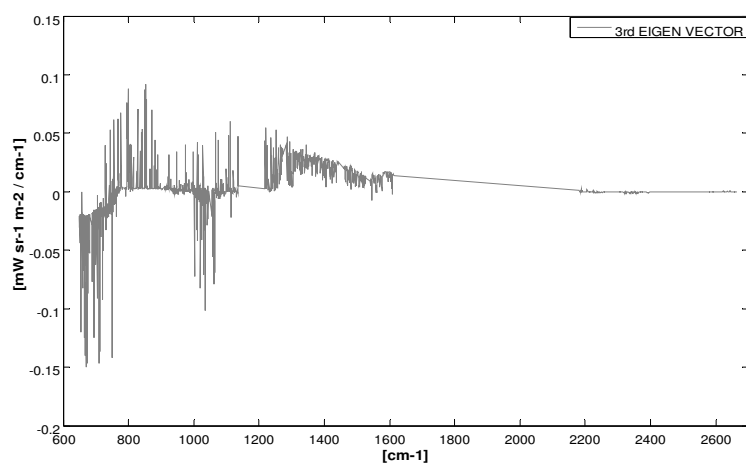
FIGURE 5.8 : First three eigen vectors derived from principal component analysis (TYPE1)



(a)



(b)



(c)

FIGURE 5.9 : First three eigen vectors derived from principal component analysis (TYPE2)

5.5. CLOSURE

An overview of various statistical tool used in the present work were described in detail. They constitute the numerical model for the retrieval of atmospheric temperature and humidity profile. Results based on retrieval by these models are discussed in the next chapter.

CHAPTER SIX

RESULTS AND DISCUSSION

6.1. RETRIEVAL OF TEMPERATURE AND HUMIDITY PROFILE

For verification of retrievals by Artificial Neural Network (ANN) model, results from linear regression are studied and compared with ANN results. For a more accurate analysis, principal components were used as predictor variables and atmospheric parameters were retrieved at each pressure layer. The behavior of the retrieval by using different number of principal components is noted to give a conclusive idea on its performance. Theoretically, by increasing the number of components, the result converges to most accurate prediction and this is evident in Principal Component (PC) based regression. For both datasets, TYPE 1 and TYPE 2, the PC based ANN and PC based linear regression retrievals were tested. In both these cases, the ANN model should perform with same accuracy as that of regression for various components.

6.1.1. TYPE1 Dataset

(a) *PC based LINEAR REGRESSION*: The temperature profile retrieval performance for linear regression is shown in FIGURE 6.1 and the water vapor retrieval performance in FIGURE 6.2 and FIGURE 6.3 . The temperature retrieval results are expressed in Root Mean Square (RMSE) Error of temperature (K) for each layer with water vapor results shown in RMSE of mass mixing ratio (g/Kg of dry air), as well as, in percentage error, where for each profile the mass mixing ratio error is weighted by the mean ratio. A bias of less than 1K was found at all pressure levels for the three cases. The accuracy of

retrieval using 500 components was more when compared with 10 or 100 components performance. It is also noted that convergence of the solution decreases as number of components increases, which implies that an optimal number of components could be sought for regression while maintaining a limit of accuracy.

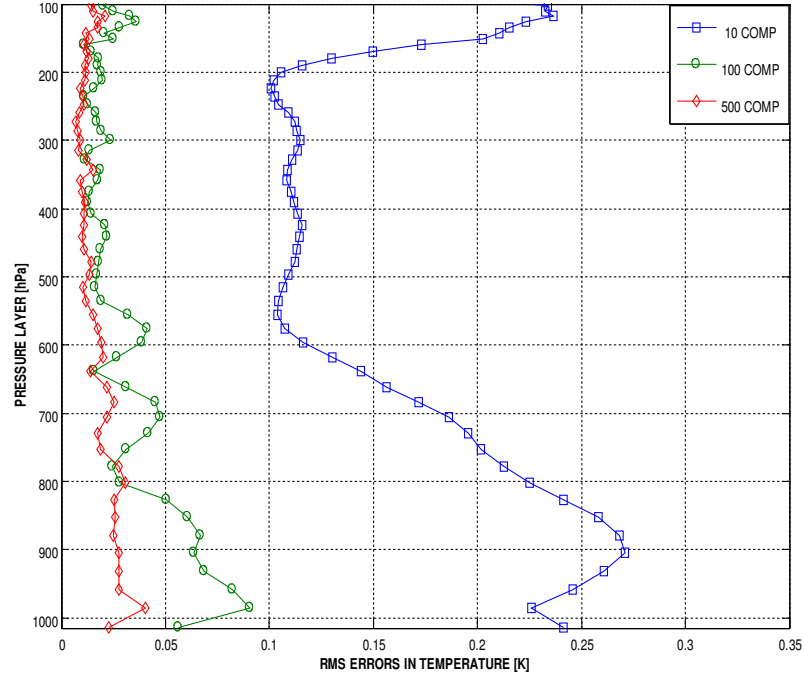


FIGURE 6.1 : Temperature retrieval performance of PC based linear regression (TYPE1)

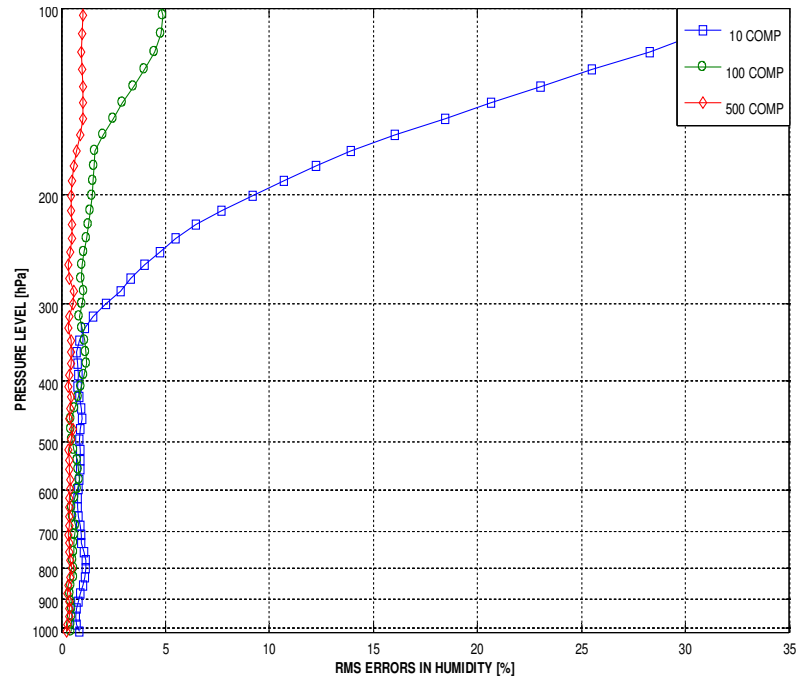


FIGURE 6.2 : Humidity retrieval performance of PC based linear regression (TYPE1)

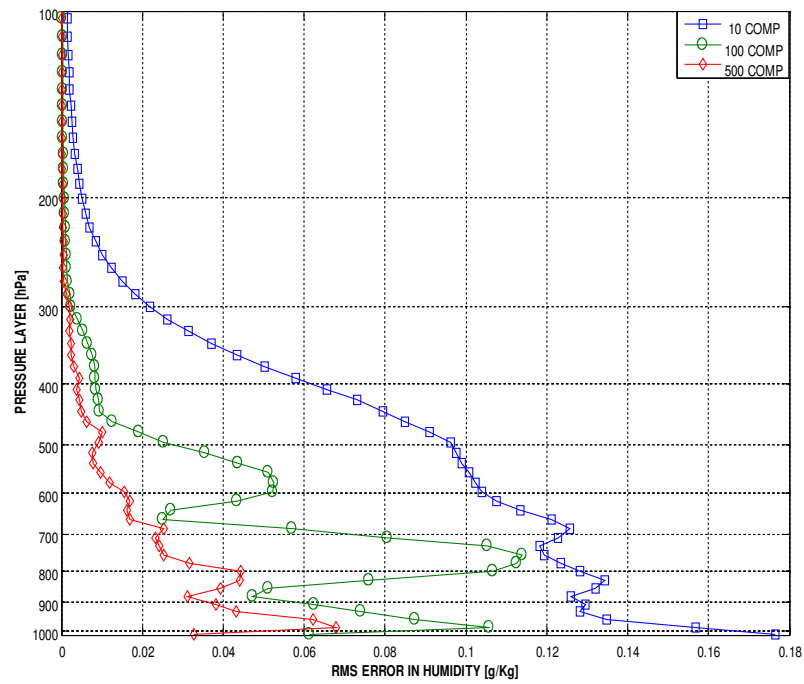


FIGURE 6.3 : Humidity retrieval performance of PC based linear regression (TYPE1)

(b) *PC based ANN*: The temperature profile retrieval performance for PC based ANN is shown in FIGURE 6.4 with the water vapor retrieval performance in FIGURE 6.5 and FIGURE 6.6 . The bias for 500 components is relatively more when compared with 100 components retrieval. Furthermore, the profile performance of water vapor retrieval for 500 components is good only up to 300 hPa. This implies that an optimal number of components exist, which leads to the most accurate prediction by ANN, for both, temperature and humidity prediction.

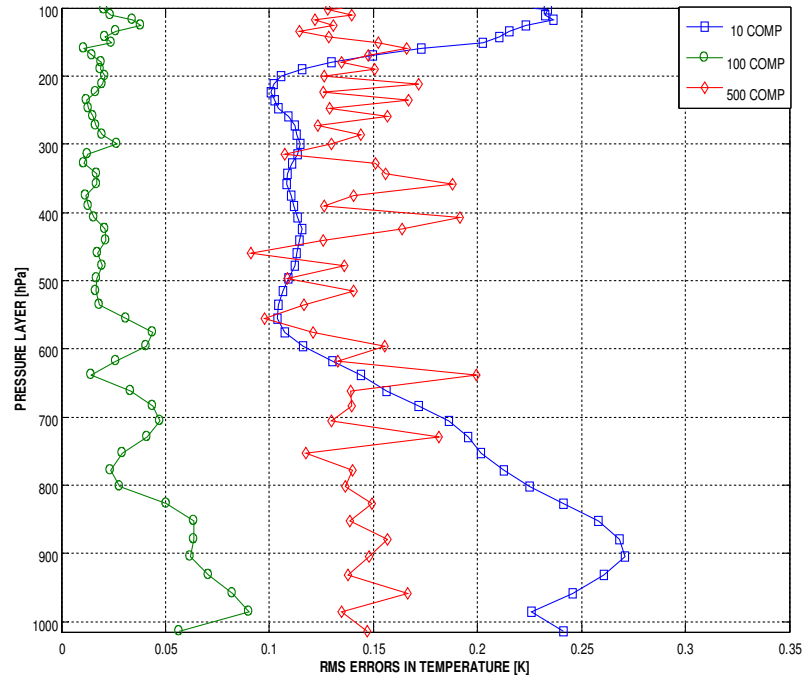


FIGURE 6.4 : Temperature retrieval performance of PC based ANN (TYPE1)

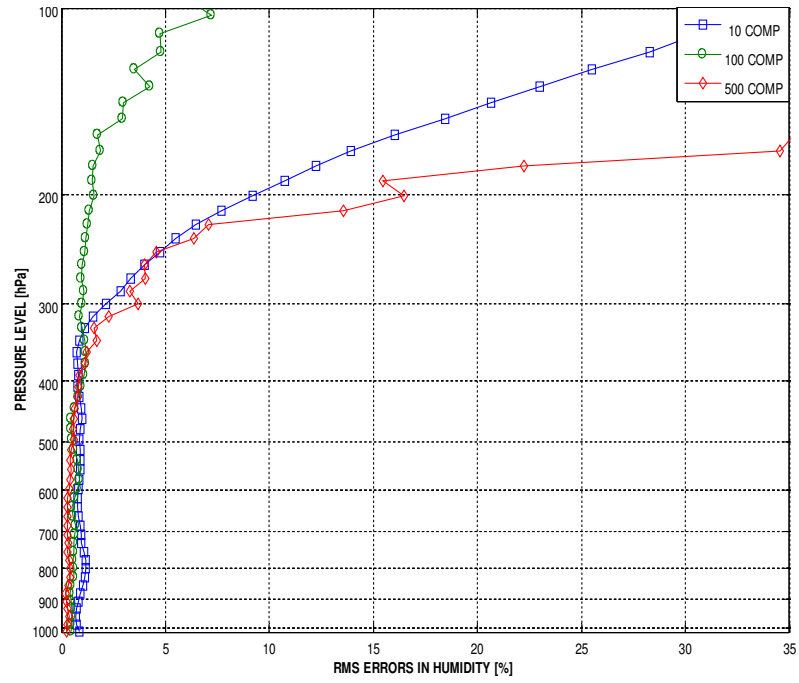


FIGURE 6.5 : Humidity retrieval performance of PC based ANN (TYPE1)

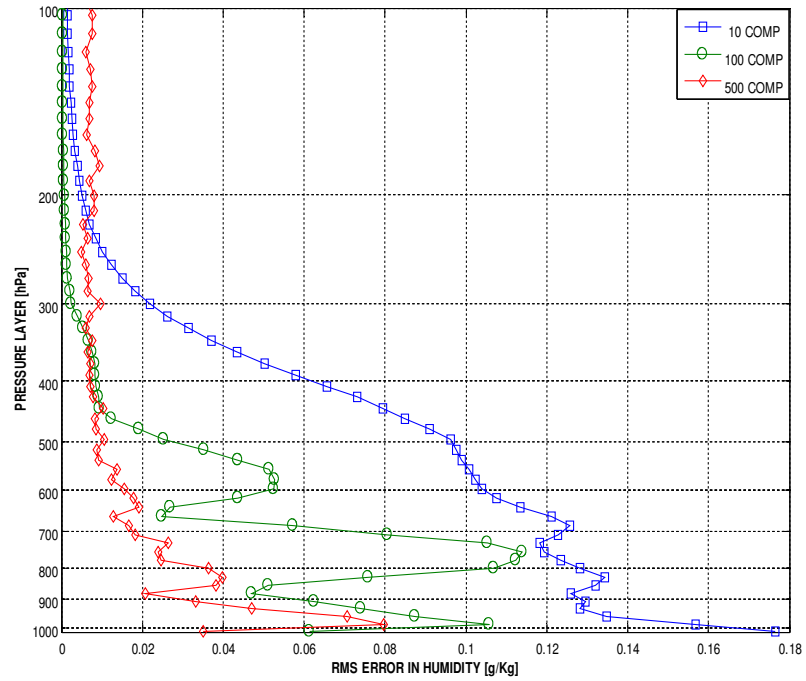
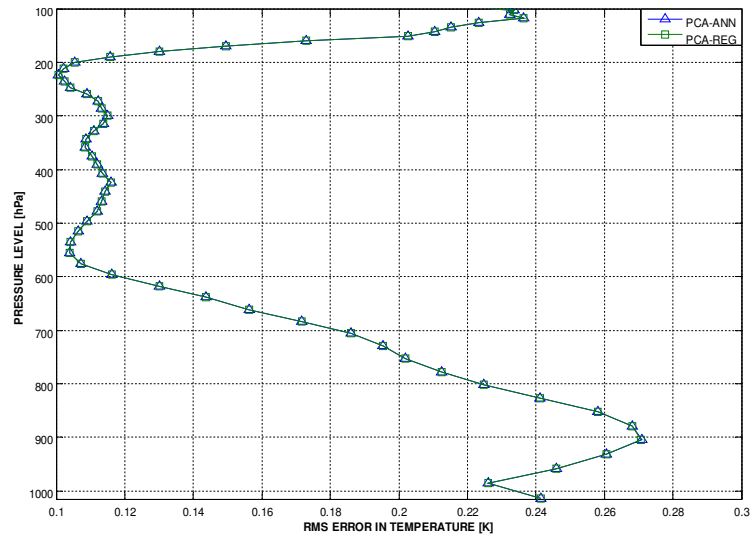
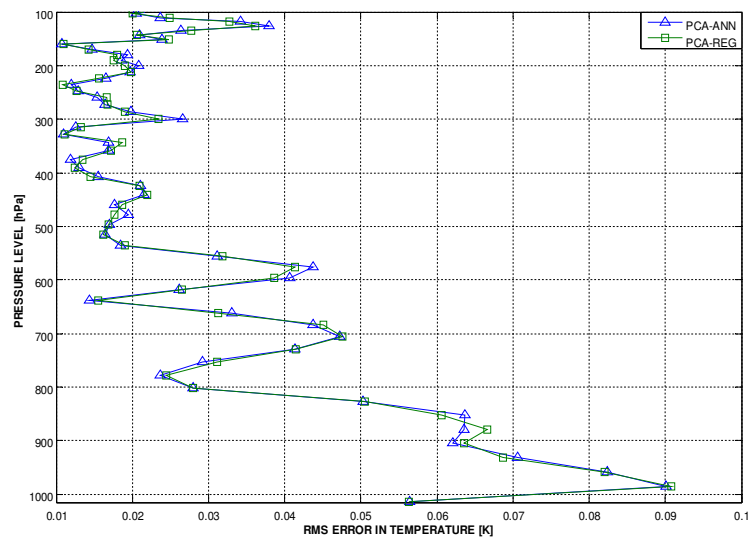


FIGURE 6.6 : Humidity retrieval performance of PC based ANN (TYPE1)

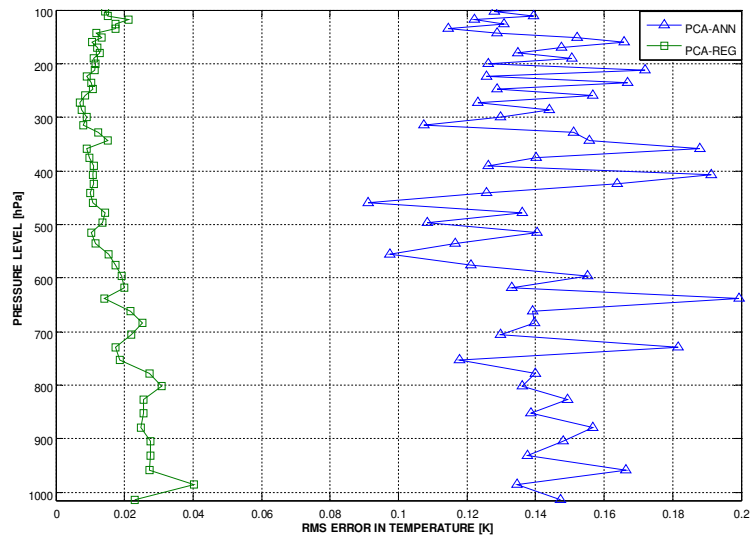
(c) *LINEAR REGRESSION versus ANN PREDICTION*: There are several features in FIGURE 6.7, 6.8 , 6.9 that are worthy of note. First, the performance of PC based ANN is comparable with the performance of PC based Linear Regression. This is primarily due to selection of components on the basis of covariance, thereby leading to an accurate prediction with the two models. Second, for lower number of components, retrieval performances of the two models coincides whereas in case of higher number of components, the regression model predicts more accurately at higher pressure level. With a large variation in the order of water vapor content (10^{-4} to 10^1), the ANN model fails to adapt to fluctuations, resulting in large error percentage. Further analyses of this discrepancy suggest that the performance of PC based ANN method for higher components is suboptimal and could be improved by choosing appropriate scheme to normalize the humidity profile.



(a)

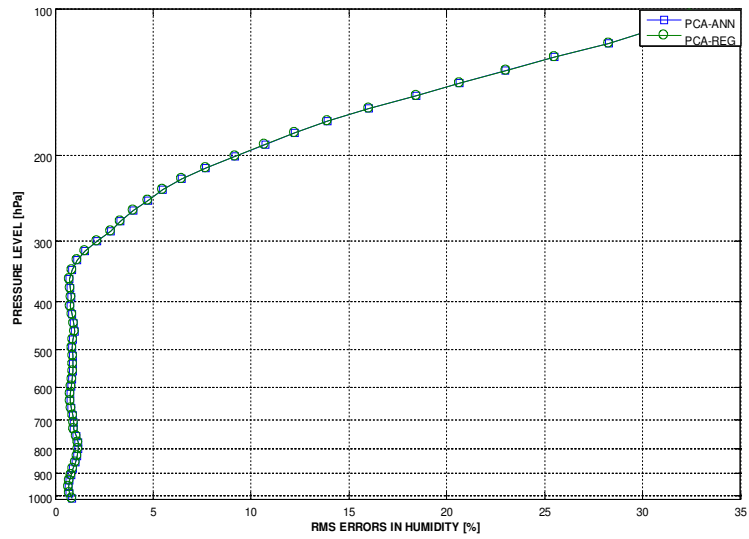


(b)

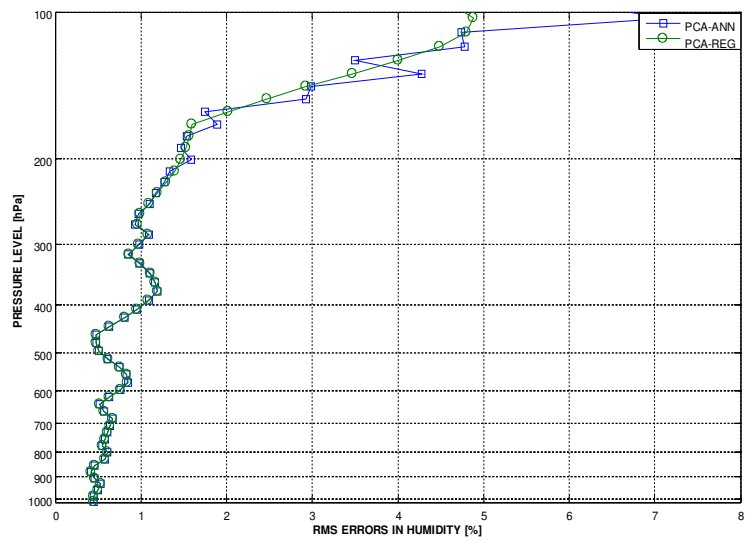


(c)

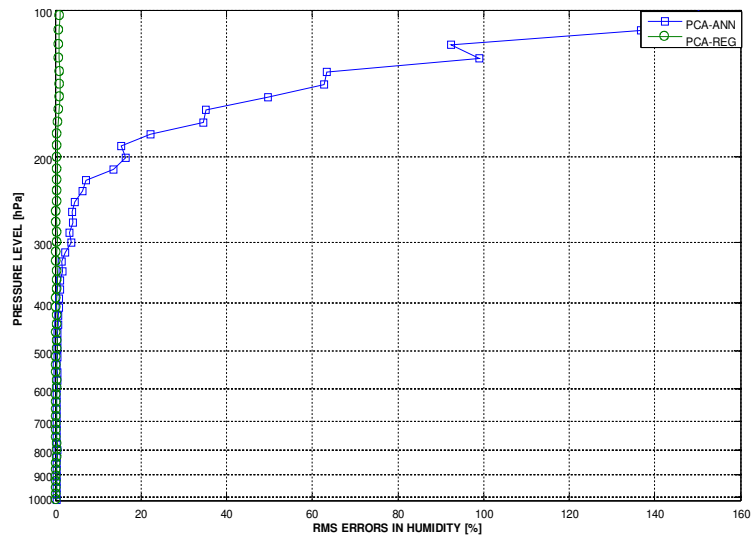
FIGURE 6.7 : Comparison of PC based linear regression with PC based ANN for temperature retrievals (TYPE1) with (a) 10 (b) 100 and (c) 500 PCs



(a)



(b)



(c)

FIGURE 6.8 : Comparison of PC based linear regression with PC based ANN for humidity retrievals (TYPE1) with (a) 10 (b) 100 and (c) 500 PCs

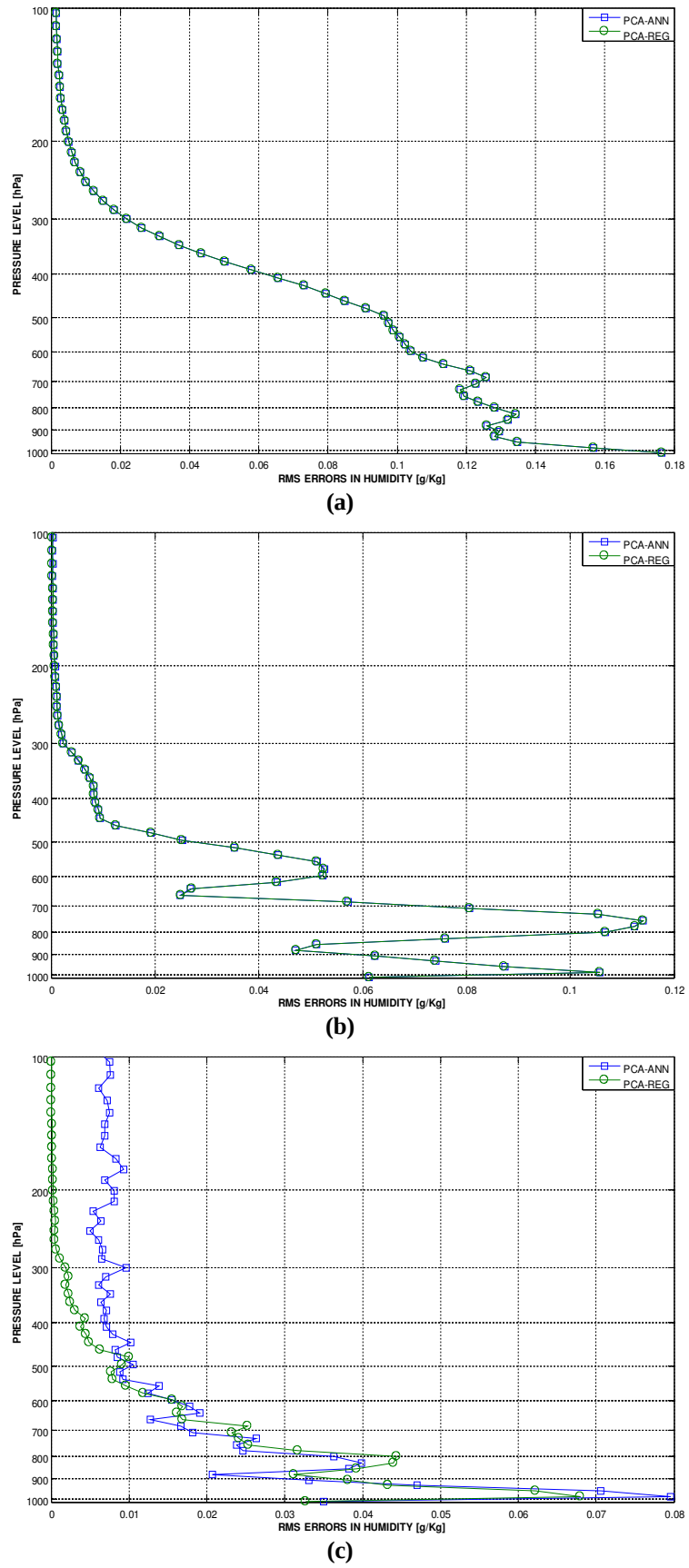


FIGURE 6.9 : Comparison of PC based linear regression with PC based ANN for humidity retrievals (TYPE1) with (a) 10 (b) 100 and (c) 500 PCs

6.1.2. TYPE2 Dataset

(a) *PC based LINEAR REGRESSION*: FIGURE 6.10 depicts the temperature profile retrieval performance for linear regression. Testing with radiosonde profiles, 10 component retrieval predicts with a bias of more than 1K. As expected, the retrieval is much better with a higher number of components, although a threshold can be achieved beyond which all the retrievals will predict within 1K mean RMS error. Water vapor retrieval performance as shown in FIGURE 6.11 and FIGURE 6.12 , are also accurate for higher number of components, but with increasing components the prediction error in higher pressure level increases rapidly.

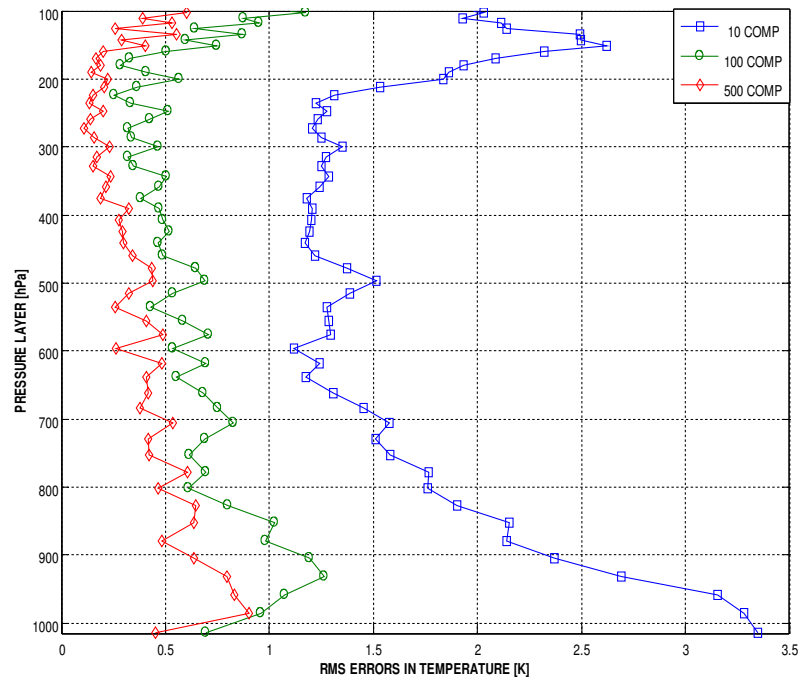


FIGURE 6.10 : Temperature retrieval performance of PC based linear regression (TYPE2)

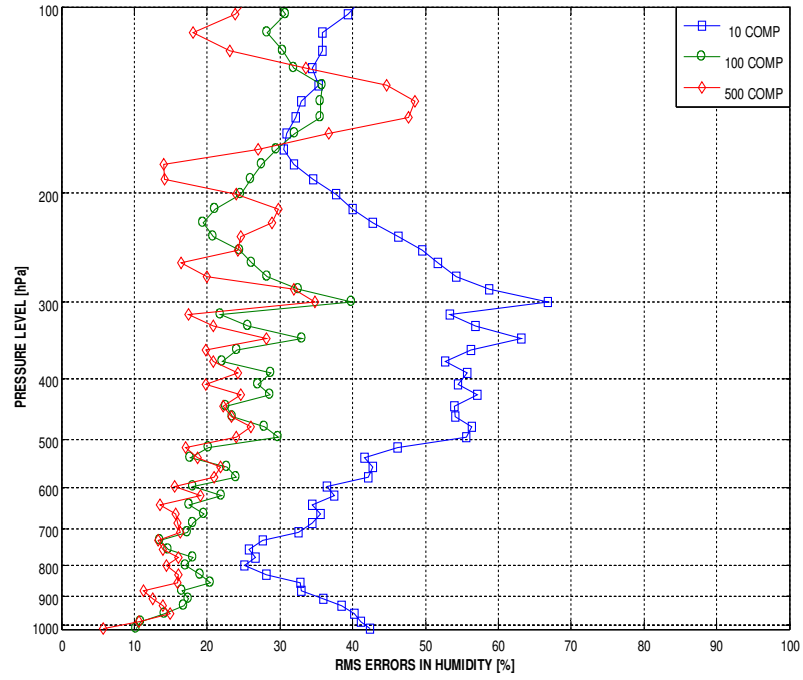


FIGURE 6.11 : Humidity retrieval performance of PC based linear regression (TYPE2)

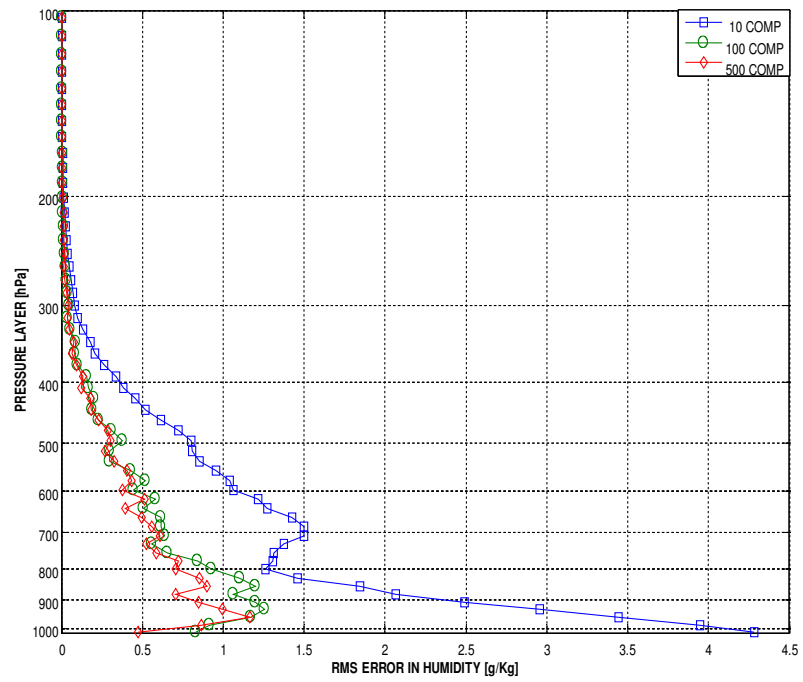


FIGURE 6.12 : Humidity retrieval performance of PC based linear regression (TYPE2)

(b) *PC based ANN*: Shown in FIGURE 6.13 , the performance follows same trend as that of TYPE1 dataset. Results for higher number of components are good when retrieving for lower pressure levels (1000hPa – 400hPa), whereas the retrieval deviates drastically for upper layers. FIGURE 6.14 and FIGURE 6.15 shows water vapor retrieval performance for PC based ANN when validated on RS profiles.

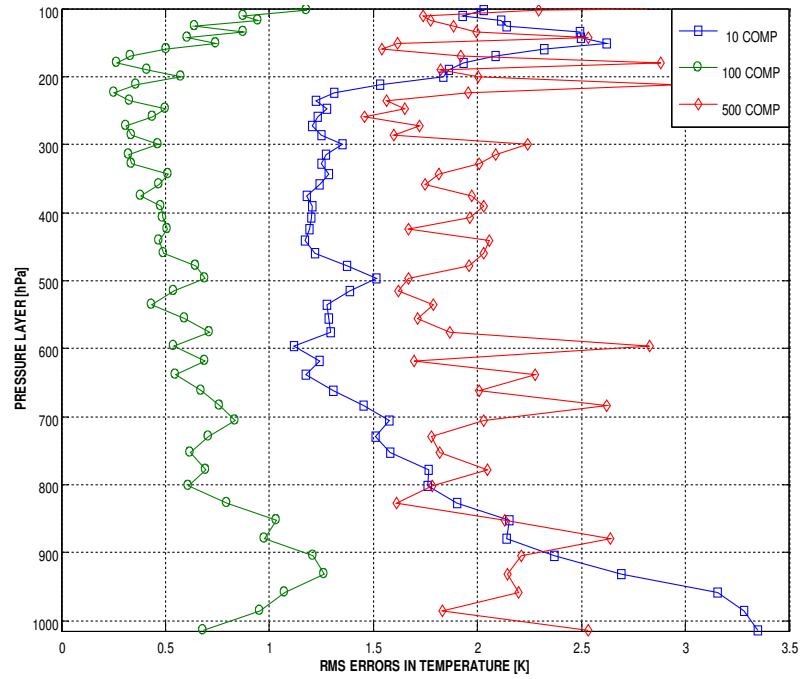


FIGURE 6.13 : Temperature retrieval performance of PC based ANN (TYPE2)

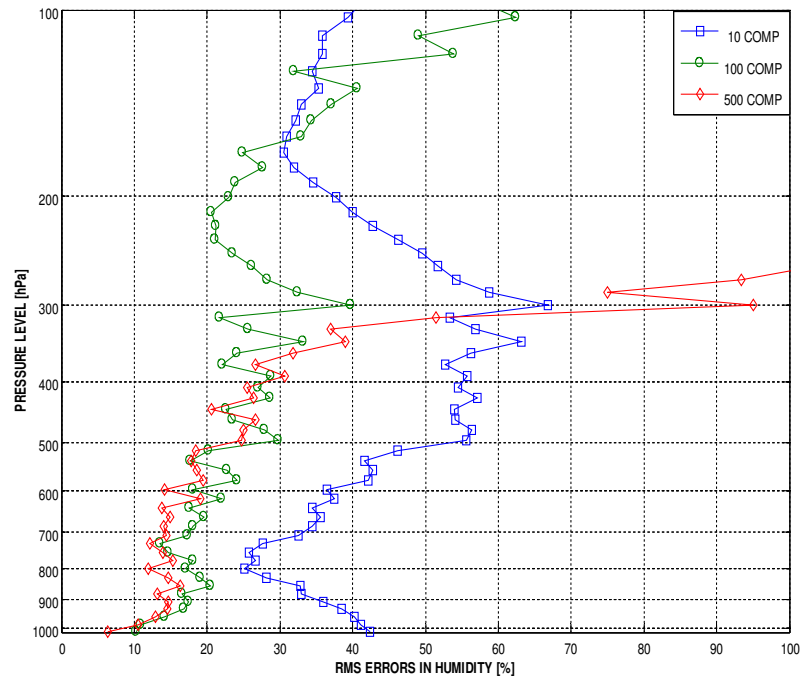


FIGURE 6.14 : Humidity retrieval performance of PC based ANN (TYPE2)

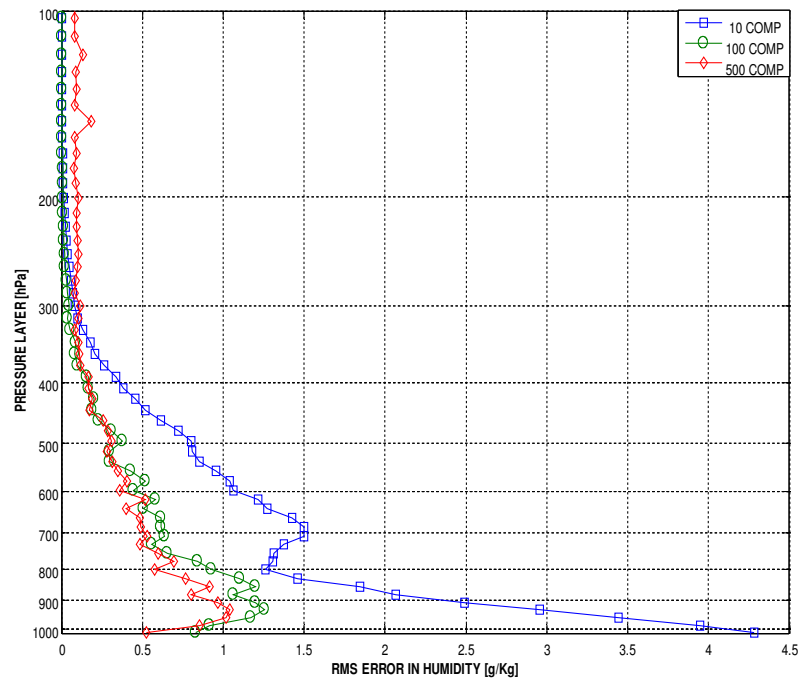
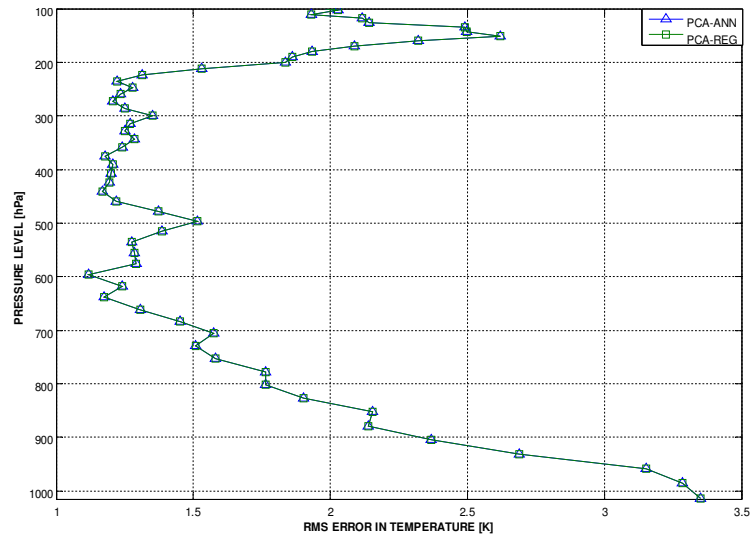
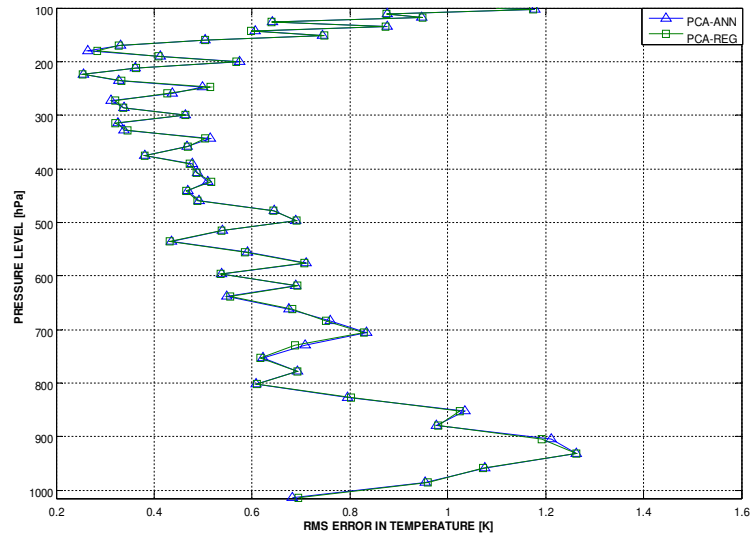


FIGURE 6.15 : Humidity retrieval performance of PC based ANN (TYPE2)

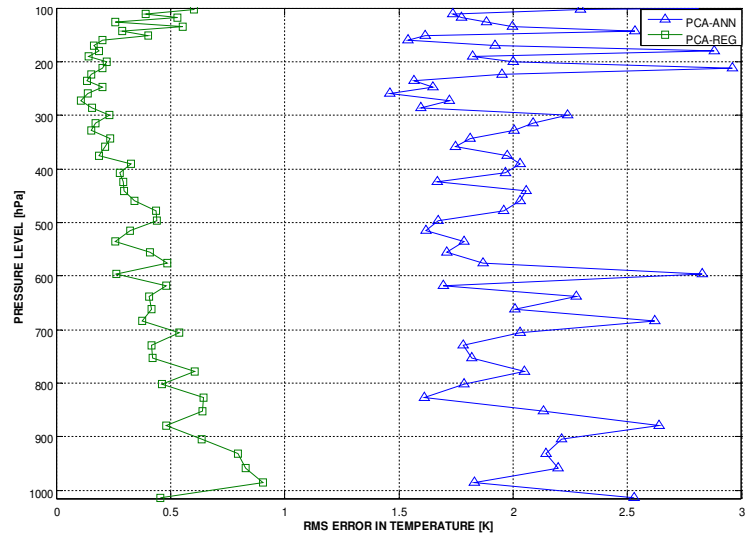
(c) *LINEAR REGRESSION versus ANN PREDICTION*: FIGURE 6.16, 6.17, 6.18 shows that the results are similar to that of TYPE1 dataset, with more erroneous performance because of realistic radiosonde profile used for validation against synthetic profile of TYPE1. The performance of 10 components ANN coincides perfectly with linear regression results, but the accuracy of the retrievals are relatively low when compared with 100 and 500 components. The 100 component ANN retrieval, on the other hand, has a slight deviation in the upper layer with regression results but gives relatively higher accuracy. This proves that there exist an optimal number of components in PC based ANN which when used will produce the most accurate retrieval using ANN model.



(a)

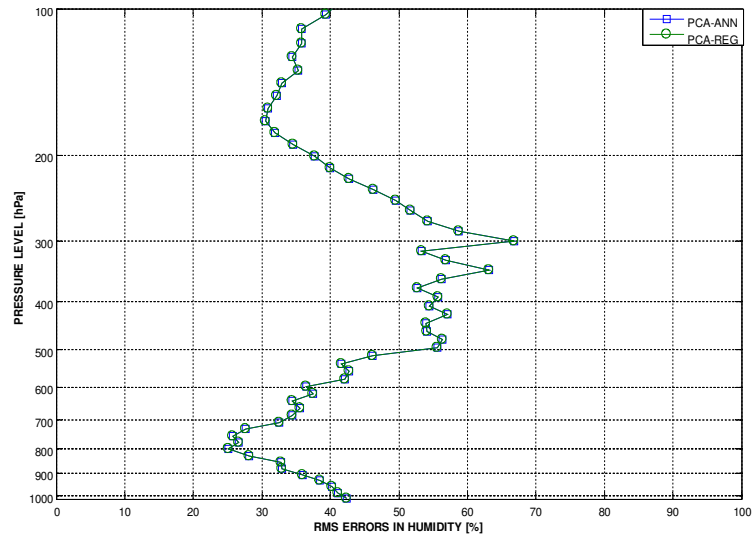


(b)

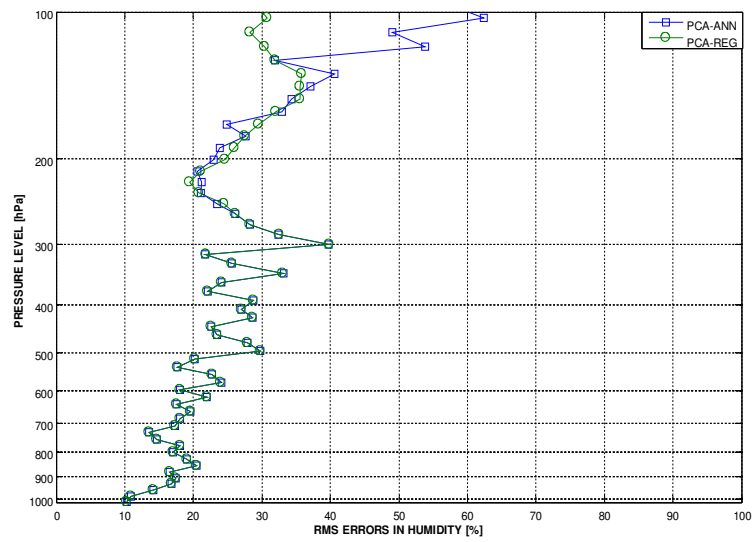


(c)

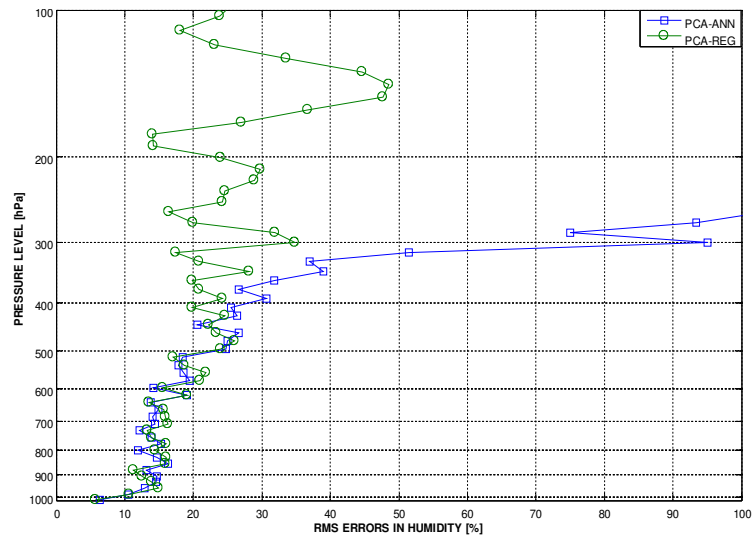
FIGURE 6.16 : Comparison of PC based linear regression with PC based ANN for temperature retrievals (TYPE2) with (a) 10 (b) 100 and (c) 500 PCs



(a)

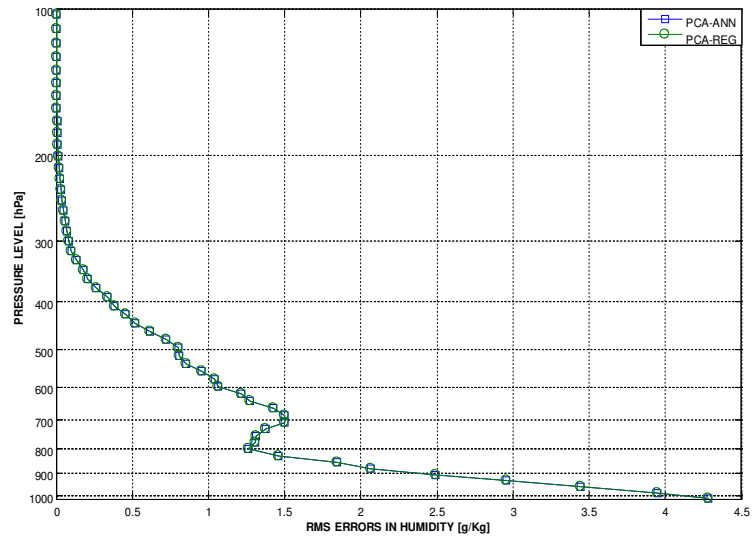


(b)

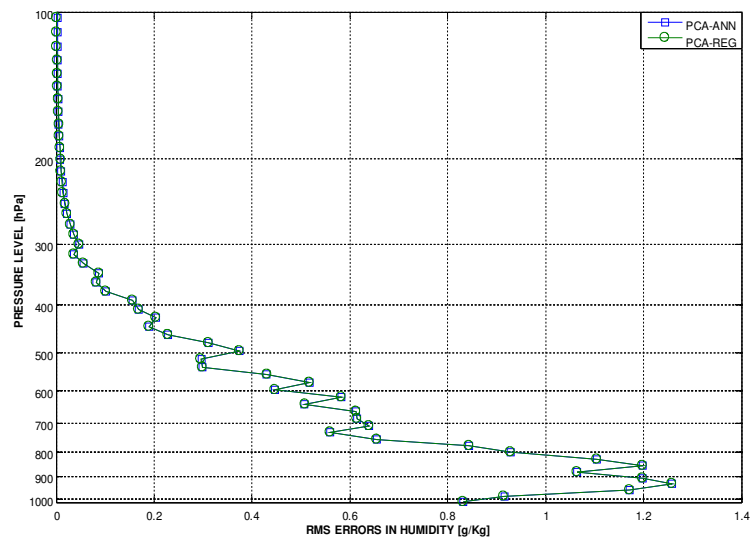


(c)

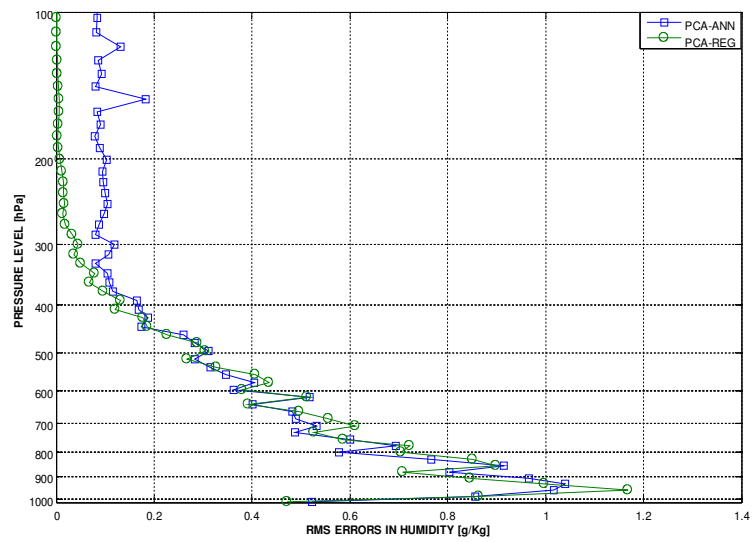
FIGURE 6.17 : Comparison of PC based linear regression with PC based ANN for humidity retrievals (TYPE2) with (a) 10 (b) 100 and (c) 500 PCs



(a)



(b)



(c)

FIGURE 6.18 : Comparison of PC based linear regression with PC based ANN for humidity retrievals (TYPE2) with (a) 10 (b) 100 and (c) 500 PCs

6.2. CLOSURE

In this chapter, the retrieval performance of statistical model are presented. The comparison between PC based regression and PC based ANN are discussed with the study of retrieval accuracy on varying numbers of PCs. The observed plots given are all numerically simulated and presented for various cases.

CHAPTER SEVEN

CONCLUSION AND SCOPE FOR FUTURE WORK

7.1. CONCLUSION

The present work of the project was divided into two main parts. The first part dealt with the applications of Principal Components (PC) in solving inverse Radiative Transfer Equation (RTE) using Artificial Neural Network (ANN) on high spectral radiance measurement. The second part was based on the comparative study of PC based linear regression with PC based ANN. The results from each part were recorded, analyzed and compared with the work previous done on this subject.

The usage of PCs as input in ANN model was proposed in this work. The main emphasize of the work was to obtain an optimal compression of high spectral infrared radiances for accurate retrieval from the ANN model trained to simulate atmospheric profiles. Results from PC based ANN were promising and the performance when varying the number of PCs were in accordance to predictions. The estimates of atmospheric temperature and humidity profiles were in accordance to the norms set by World Meteorological Organization i.e. less than 1K mean RMSE and 20% - 30% mean RMSE for humidity retrieval.

PC based regression were also used for comparing its performance with PC based ANN. It was found that the retrieval of the two matched perfectly for smaller number of PCs, where as it deviated drastically as number of PCs were increased. For many cases, it has

been shown that simple ANN model performs better in comparison to linear regression. In contrast, PC based regression retrieval was better than ANN retrieval in this case, even when tested with realist dataset TYPE2. The ANN prediction for higher altitudes, typically 300mbar–100mbar, were more deviated than regression prediction which implies that non-linear ANN models are required for accurate retrieval.

Evaluation of PC based ANN for the retrieval of atmospheric temperature / humidity profile form the crux of the present work. Results of the analysis are encouraging for studying the application of advance PC methods on ANN model. Hence, PC based ANN promises to be an effective tool in compressing high dimensional radiance measurement and retrieving temperature and humidity profile with precision.

7.2. SUGGESTIONS FOR FUTURE WORK

The retrieval results demonstrated effectiveness and robustness of the algorithms used. Although, further improvement to the retrievals can be achieved. Throughout the course of work, all channels of the Atmospheric Infrared Sounder (AIRS) were given equal weightage to extract maximum geophysical parameters. This could be improved by selecting those channels which are characteristic of certain atmospheric constituents, in this case H_2O (water vapor). Certain datasets like NOAA-88b radiosonde profile, SeeBor-V4.0 dataset compiled specifically for training purposes, can be included in this analysis . These datasets, if used will increase generalization of the model, leading to better prediction for realistic profiles. Various normalizing factors like logarithmic humidity profiles, can be tested to reduce the deviation of retrieved humidity profile. The efficiency of the ANN model can be improved by implementing new architecture to the

neural network, like radial basis functions as activation functions. They are capable of time series prediction, function approximation and control and thereby can handle chaotic data better than other conventional functions. These functions if used, will give smoother and more stable retrieved profiles, similar to clear sky conditions in the atmosphere.

For developing a highly robust retrieval algorithm, realistic radiances can be implemented in the model by adding Noise Effective Temperature Difference ($NE\Delta T$) errors to the brightness temperature simulated by kCARTA. These radiances will improve the generalization of ANN and together with kCARTA forward model will provide reliable, ground truth dataset for other retrieval models.

REFERENCES

- [1] Aires, F.¹ , W. B. Rossow, N. A. Scott, and A. Chédin, 2002: Remote sensing from the infrared atmospheric sounding interferometer instrument: 1. Compression, denoising, first-guess retrieval inversion algorithms, *Journal of Geophysical Research*, **107(D22)**, 4619.
- [2] Aires, F.² , W. B. Rossow, N. A. Scott, and A. Chédin, 2002: Remote sensing from the infrared atmospheric sounding interferometer instrument: 2. Simultaneous retrieval of temperature, water vapor, and ozone atmospheric profiles, *Journal of Geophysical Research*, **107(D22)**, 4620.
- [3] Blackwell, W. , J. , 2005: A neural-network technique for the retrieval of atmospheric temperature and moisture profiles from high spectral resolution sounding data. *IEEE Transaction on Geoscience and Remote Sensing*, **43**, No. 11.
- [4] De Souza-Machado, S., L. Strow, and S. Hannon, 1997: kCompressed atmospheric radiative transfer algorithm (kCARTA). *Satellite Remote Sensing Wavenumber (cm^{-1}) of Clouds and the Atmosphere, Proceedings of the European Symposium on Aerospace Remote Sensing 3220, Europto Series, Institute of Electrical Engineers, London, Great Britain.*
- [5] Demuth, H. , M. Beale, M. Hagan, 2009: Neural Network Toolbox™ 6, User's Guide, MATLAB® , © COPYRIGHT 1992–2009 by The Math Works™, Inc.

- [6] **Escobar-Munoz, J. , A. Chedin, F. Cheruy, and N. Scott**, 1993: Reseaux de neurones multicouches pour la restitution de variables thermodynamiques atmosphériques à l'aide de sondeurs verticaux satellitaires. *Comptes-Rendus de L'Academie Des Sciences; Série II*, **317(7)**, 911–918.
- [7] **Hannon, S. E. , L. L. Strow, and W. W. McMillan**, 1996: Atmospheric infrared fast transmittance models: A comparison of two approaches. In *Proceedings of SPIE Conference 2830, Optical Spectroscopic Techniques and Instrumentation for Atmospheric and Space Research II*.
- [8] **Huang, H. L. , and P. Antonelli**, 2001: Application of principal component analysis to high-resolution infrared measurement compression and retrieval, *Journal of Climate and Applied Meteorology*, **40**, 365–388.
- [9] **Strow, L. L. , H. E. Motteler, R. G. Benson, S. E. Hannon and S. De Souza-Machado**, 1998: Fast Computation of Monochromatic Infrared Atmospheric Transmittances Using Compressed Look-Up Tables, *Journal of Quantitative Spectroscopy and Radiative Transfer*, **59(3-5)**, 481–493
- [10] **Xuebao, W. , L. Jun, Z. Wenjian and W. Fang**, 2005: Atmospheric Profile Retrieval with AIRS Data and Validation at the ARM CART Site, *Advances in Atmospheric Sciences*, **22(5)**, 647-654.